ChemSystemsChem

Review
doi.org/10.1002/syst.202400101

Chemistry Europe
European Chemical Societies Publishing

www.chemsystemschem.org

Autonomous Artificial Molecular Motors and Pumps

Chiara Taticchi,[a, b] Massimiliano Curcio,[a, b] and Stefano Corra*[a, b]

Over the past decade there has been a tremendous development of systems capable to autonomously convert energy, in particular light and chemical, into directed motion at the nanoscale. These nanoscopic devices are called molecular motors. The autonomous operation of artificial molecular motors and pumps under constant experimental conditions represents a key achievement to their implementation into more sophisticated networks. Nonetheless, the principles behind successful autonomous operation are only recently being rationalized. Within this review we focus on the fundamental aspects that enable the autonomous operation of molecular motors exploiting light and chemical energy. We also compare the mechanisms of operation with these two energy sources and highlight the common ground of these systems as well as their differences and specificities by discussing a selection of recent examples in the two classes. Finally, we provide a perspective view on future advances in this exciting research area.

1. Introduction

The importance of autonomously converting energy into directional motion at the molecular level can be hardly overestimated. Nature addresses this task through molecular motors (or engines) and pumps, a particular type of molecular machines capable of continuously and autonomously use an energy source to achieve directional movement and sustain concentration gradients.[1] Motor proteins and pumps are exploited in living systems to perform a wide range of fundamental tasks, from cargo transport to DNA replication, to motility. They can use energy, in the form of ATP hydrolysis, to bias the diffusion along a track (microtubule, DNA filament) or to rotate in a preferred direction about their axis moving a flagellum that provides propulsion into aqueous media.[2] Similarly, light or ATP hydrolysis can be used to bias the concentration of ions across a membrane generating gradients that can be exploited for other chemical processes downhill.[3,4] All these molecular motors work in environmental conditions that enable steady state operation, namely a sufficiently higher concentration of fuel (ATP or other chemical fuel) with respect to the motor or stable spectral radiant power of light.[5] Over the last twenty to thirty years, there has been a growing interest in preparing artificial systems capable of controlling the mechanical-like movements of the (sub)molecular components using energy from an external source, namely artificial molecular motors and pumps. However, achieving an operational steady state sustained by the continuous consumption of energy from a stable external source (i.e. autonomous operation) has emerged as one of the main challenges in the design of these artificial systems. Autonomous operation is, in fact, a highly desirable characteristic not only for the limited operator intervention, but more importantly to introduce these active systems into complex environments (e.g., a cell), and to enable their integration into elaborate multi-process cascades, similarly to what happens in living systems.[1–4,6]

In general, chemical, light, or electrical energy have been used to drive molecular motors and pumps. However, so far only chemical fuels and light have been successfully applied to drive motors and pumps autonomously. This characteristic is mostly due to their intrinsic operation mechanisms.

Within this short review we discuss the general operation mechanism of autonomous molecular motors using light or chemical energy input—also referred as "fuel"—highlighting the common ground behind their operation as well as their specificities. We discuss a selection of the major advancements in this field over the last 10 years with a focus on those works that expanded the playground of motors in terms of chemical network topologies or investigation. Finally, we provide some prospective avenues for future research directions. The systems operating with "fuel" pulses, such as those driven by alternating or pulsed electrochemical potential,[7,8] uncatalyzed fuel decomposition (e.g., activated carboxylic acids),[9] or bistable photoswitches that need dual wavelength inputs,[10] albeit interesting and also challenging, are not able to operate in a stationary state, and therefore are outside the scope of this review. Similarly, prospective applications of some of the described motors have been reviewed elsewhere.[10,11]

2. Ratcheting Brownian Motion

Like their macroscopic counterparts, molecular motors operate by continuously going through a closed sequence of transformations that can be repeated indefinitely and realize unidirectional

[a] Dr. C. Taticchi, Dr. M. Curcio, Dr. S. Corra
Department of Industrial Chemistry "Toso-Montanari", University of Bologna, Via P. Gobetti 85, Bologna 40129, Italy
E-mail: stefano.corra@unibo.it

[b] Dr. C. Taticchi, Dr. M. Curcio, Dr. S. Corra
Center for Light Activated Nanostructures, CNR-Institute for Organic Chemistry and Photoreactivity, Via P. Gobetti 101, Bologna 40129, Italy

motion of one component with respect to the other. Although, this can be easily achieved in the macroscopic world—where Newtonian physics holds true—in the nanoscopic domain, it is not a straightforward task. At the molecular level, in fact, thermal energy results in an endless "jiggling" of the atoms which disrupts any directionality. This agitation is commonly referred to as "Brownian motion" and to achieve directional movement it is necessary to bias this random motion.[12] This is obtained through ratchet mechanisms, which exploit an external energy source to break spatial and time-reversal symmetries along the direction of motion with the application of a time-dependent potential with repeating asymmetric features.[13,14] The categories of ratchets of interest in the context of molecular motors are *energy* and *information ratchets*; their detailed description is beyond the scope of the current perspective and have been extensively discussed elsewhere.[10,13,14] Here, we will limit our explanation to saying that energy ratchets (Figure 1a) asymmetrically modulate both energy maxima (kinetics) and minima (thermodynamics), whereas information ratchets (Figure 1b) modulate only the energy maxima depending on the position of the Brownian particle.

Practically, the reaction scheme realizing the ratchet at the basis of all artificial molecular motors involves coupling a set of *energy harvesting reactions* (processes *2* and *4* in Figure 2a), along with suitable *reciprocal reactions* performing the opposite transformation to close the cycle (processes *2′* and *4′* in Figure 2a), with a set of *isomerization processes* that provide the mechanical motion (processes *1* and *3* in Figure 2a).[15] Since each reaction typically interconverts two states (Figure 1c,d), the general result is a four-membered closed reaction network (square scheme, Figure 2a) in which the energy harvesting processes drive the isomerization reactions. During operation, detailed balance cannot be fulfilled, the system thus reaches a steady state away from thermodynamic equilibrium and uses energy to sustain it while rectifying the Brownian motion of the "mechanical" isomerization.[15] The operational steady state is determined by the *kinetic asymmetry* of the closed reaction cycle. Kinetic asymmetry is quantified by the ratcheting constant that can be defined as the ratio between the product of the rates for all semireactions taken in the clockwise cycling direction (Figure 2b, left) and the product of the rates for the reverse counterclockwise semireactions (Figure 2b, right).[16] For a four-stage reaction cycle like the one in Figure 2a the ratcheting constant (K_r) is:

$$K_r = \frac{r_1}{r_{-1}} \times \frac{r_2 + r_{2'}}{r_{-2} + r_{-2'}} \times \frac{r_{-3}}{r_3} \times \frac{r_{-4} + r_{-4'}}{r_4 + r_{4'}} \quad (1)$$

When $K_r > 1$ (or < 1) detailed balance is broken, the system cannot relax to thermodynamic equilibrium, and the network is continuously travelled clockwise (or counterclockwise).[15]

These general principles of operation are conceptually similar for any molecular motor, regardless of the energy source.[13,14,17,18] There are, however, minor specificities related to the energy source employed to drive the motor, or to the nature of the energy-harvesting process. These specificities, as well as the

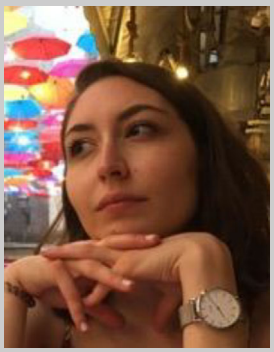

Chiara Taticchi received her M.Sc. in photochemistry and molecular materials magna cum laude in 2019 under the supervision of Prof. Alberto Credi at the University of Bologna. She later pursued doctoral studies in the same research group, earning her PhD in chemistry in 2023. Since then, she has been a postdoctoral researcher in the same group. Her research focuses on the characterization of artificial molecular machines based on mechanically interlocked molecules (MIMs) and photochromic systems for the development of light-effected materials.

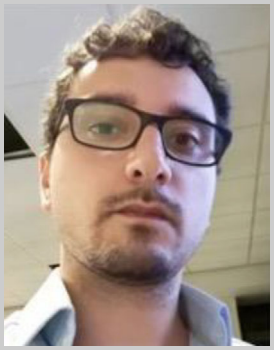

Massimiliano Curcio (Max) completed his doctoral studies at the University of Edinburgh, developing redox-active ligands for electron transfer reactions and defending his thesis in late 2018. After a research stay at the Technical University of Munich, in 2019 Max moved to Bologna as a postdoctoral fellow to acquire expertise in the field of artificial molecular machines. Since 2023, Max is an assistant professor at the University of Bologna, working at the intersection between molecular and supramolecular chemistry with a focus on motion control at the nanoscale and on the coordination chemistry of unconventional heterocyclic compounds.

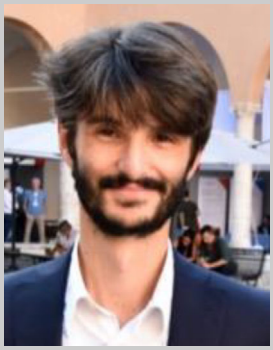

Stefano Corrà graduated in industrial chemistry from the University of Padova under the supervision of Prof. Paolo Scrimin and Leonard Prins (2012). He later moved to ETH for his PhD studies in the group of Prof Helma Wennemers and graduated in 2018 with a thesis on peptides as scaffolds for nanotechnology. He later joined the group of Prof. Alberto Credi at the University of Bologna as a postdoctoral fellow working on light fueled supramolecular pumps. Since 2022, he became assistant professor at the same university. His research focuses on the development of bioinspired photoactive and dissipative supramolecular systems.

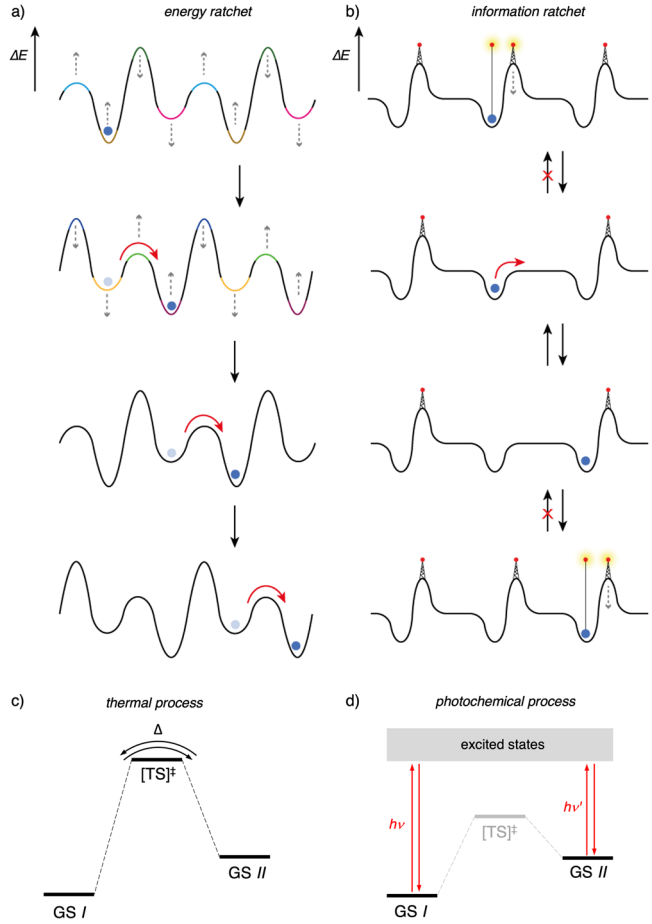

Figure 1. (a) Schematic modulation of the potential energy surface for an energy ratchet and (b) an information ratchet. Adapted with permission from ref. [10b]. Copyright 2020, American Chemical Society. The Brownian particle is represented by the blue dot. (c) Simplified energy diagrams of photochemical and (d) thermal processes. GS indicates the ground states. For the thermal processes, TS indicates the transition state. For the photochemical processes, the excited states are indicated by the grey box and excitation and relaxation are indicated by red arrows.

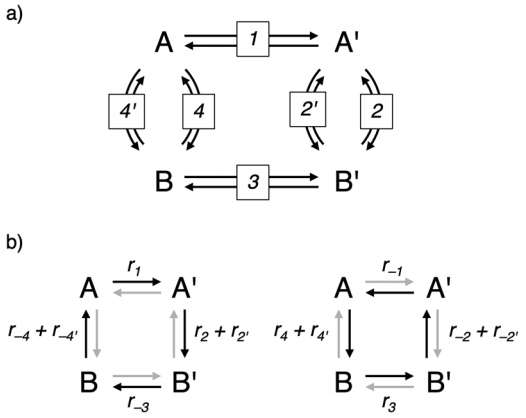

Figure 2. (a) General four-step reaction network for describing the operation of a molecular motor. Horizontal processes (1 and 3) are the ratcheted "mechanical" isomerization, vertical processes are energy harvesting (2 and 4) and their reciprocal transformations (2′ and 4′). (b) Simplified schemes for clockwise (left) and counterclockwise (right) cycling semireactions (black arrows). Rates are conventionally taken as positive from left to right and from top to bottom; for the catalytic cycles the overall forward and backward transformation rates are considered.

related challenges, will be discussed in the sections dedicated to light- and chemically-operated molecular motors.

3. Light-Fueled Molecular Motors and Pumps

Compared to other energy sources, the use of light provides exquisite spatiotemporal control, it can avoid the formation of waste products in solution upon operation, and it has the highest potential for renewability. In principle, sunlight could be used directly to power these nanomachines.[19–21] In Nature, systems based on light absorption are fundamental in two main contexts: (i) fixing carbon in an organic form that can be used by heterotroph organisms (carbohydrates), and (ii) enabling vision in animals by coupling photoisomerization of retinal in proteins to proton pumping.[22] The vision process, in particular, represented the main inspiration for the development of light-driven molecular motors. These systems, however, are mostly restricted to these two very specific tasks due to some intrinsic limitations, such as the dependency on daylight and the limited lifetimes of the excited states that affect the efficiencies of photonic phenomena (quantum yields).[23–25]

3.1. Operating Principles

This class of motors harvests light energy through photochemical reactions to drive the motor. In the most common case, the closed network of reactions involves two mechanical isomerization processes (reactions *1* and *3* in Figure 3a) and two energy harvesting photochemical reactions (reactions *2* and *4*, red arrows, termed "$h\nu$" in Figure 3a). Photonic processes proceed through an excited state (Figure 1d) whose population is dictated by Einstein coefficients for absorption and emission of light.[26] As a consequence, for a photoreaction, the composition (i.e. the product/reactant concentration ratio) at the photostationary state (PSS) is determined by the photoreaction quantum yields (governed solely by the profile of the excited-state potential energy surface) and the molar absorption coefficients. A third set of thermal reactions (*2′* and *4′*, black arrows, termed "Δ" in Figure 3a) that interconvert the photoswitches can be present. Photochemical reactions proceed via an excited state (Figure 1d) and are, thus, not bound to the constraints of microscopic reversibility which, instead, regulate thermally activated processes (Figure 1c,d).[14,23–25] For this reason, the reciprocal reactions needed to reset the system and close the cycle can be the opposite photochemical process (vertical red arrows in Figure 3a). The only practical requirement is that the forward and backward photochemical steps are triggered by photons of the same wavelength with a different quantum yield (ϕ) or molar absorptivity (ε). The presence of a third (thermal) reciprocal reaction that occur simultaneously is not a strict requirement ($k_i^{\Delta} << F_{h\nu} \cdot \phi \cdot \varepsilon$). This is extremely advantageous to implement autonomous operation under constant illumination. In turns, this also means that operation of these motors is not related to specific photophysical parameters other than the ability to absorb photons of the provided wavelength. The "easiness" for light-

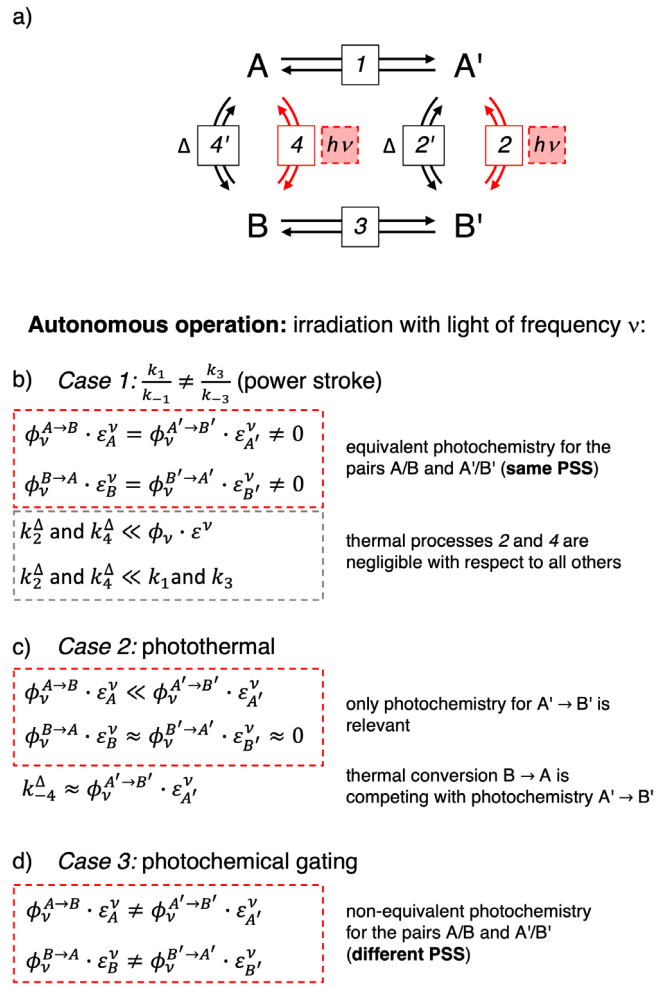

Figure 3. (a) Four-step light-fueled molecular motor ratcheting the motion of the horizontal steps. Red arrows indicate photochemical processes ($h\nu$) that proceed through an excited state (not shown), black arrows indicate thermal processes (Δ). Different limiting modes of autonomous operation involve (b) active forward and backward photochemical processes at the same wavelength and different relative stability of the A′ and B′ isomers (power stroke), (c) one active photochemical and one thermal reciprocal process proceeding with comparable rates, and (d) active forward and backward photochemical processes at the same wavelength with distinct photokinetics (photochemical gating). The ν index indicates that the photophysical parameter is referred to the frequency of irradiation (ν). For quantum yields (ϕ) the photoconversion process of reference is specified in the superscript. The superscript Δ indicates that the rate constant is referred to a thermal process "reciprocal" to a photoconversion.

related phenomena to escape microscopic reversibility is also the reason why light-driven molecular motors were the first to be synthesized by scientists.[27]

Additionally, the possibility to detour into a high energy excited state opens up interesting possibilities for motion mechanisms (but not only) not accessible at the ground state, widening largely the possible network topologies through which the motor can operate.[28,29] In the most compact designs, the number of reactions in the network has been reduced down to two, as demonstrated by Lehn for imine-based rotary motors, and more recently proposed by Olivucci with a pyrrolidinone architecture.[30,31] Similarly, the operational cycle can be expanded to more than four steps, as shown by Dube.[32] These particular cases will be discussed in detail in the following section.

In order to realize a ratcheting system, detailed balance must be broken for the network of reactions. The ratcheting constant (i.e. kinetic asymmetry, Equation 2) for a photochemical network like the one in Figure 3a, irradiated with monochromatic light, can be written by rearranging Equation (1). Standard photokinetic and mass action laws can be used to define the rates of the photochemical and thermal reactions.[33,34]

$$K_r = \frac{k_1}{k_{-1}} \times \frac{F_{h\nu}\phi^{A'\to B'}\varepsilon_{A'} + k_{2'}^\Delta}{F_{h\nu}\phi^{B'\to A'}\varepsilon_{B'} + k_{-2'}^\Delta} \times \frac{k_{-3}}{k_3} \times \frac{F_{h\nu}\phi^{B\to A}\varepsilon_B + k_{-4'}^\Delta}{F_{h\nu}\phi^{A\to B}\varepsilon_A + k_{4'}^\Delta} \qquad (2)$$

From Equation (2), it becomes evident that $K_r \neq 1$ in three limiting cases. The first possibility is that the "mechanical" isomerization steps display different equilibrium constants ($k_1/k_{-1} \neq k_3/k_{-3}$), whereas the energy harvesting steps can be equivalent for the two sets of mechanical isomers (A/B and A′/B′). The photokinetic factor ($F_{h\nu}$), the molar absorptivity (ε) and photoconversion quantum yields (ϕ), as well as the thermal isomerization steps (k_i^Δ) can be equal for the two sets of mechanical isomers (Figure 3b). In other words, this mode of operation necessitates a fast, large-range, energetically downhill molecular rearrangement step, called *power stroke*.[17,35]

A second, less explored, option for autonomous operation of light-fueled motors is to have a thermal process reverse of the photochemical one, kinetically competing with it (Figure 3c). In this way the energy dissipating cycle, that is the set of reciprocal reactions harvesting energy and resetting the system, involves one photochemical and one thermal reaction for at least one of the mechanical isomers pair. In this case, the unbalance of the populations needed to break the detailed balance can be realized in the energy harvesting steps (vertical arrows in Figure 3a). For this reason, for networks involving more than two reactions, there is no need for a power stroke in the "mechanical" isomerization steps.

The third case is that the two mechanical isomers have different photoreactivity at the irradiation wavelength (Figure 3d). In this case the PSSs are different for the two photoactive pairs. The system behaves as an information ratchet where the mechanical isomers are photoconverted with different photokinetics thanks to distinct ε and/or ϕ that are dependent on the mechanical state (photochemical gating). This mode of operation is purely kinetic and does not require a power stroke, therefore the "mechanical" isomerization steps can display the same equilibrium constants.

It is thus clear that the challenge in light-driven systems lies in the coupling between photochemical and thermal rearrangement processes. The fundamentally different physical laws behind these processes impact their timescale and render the balancing of the kinetics difficult. Moreover, as molecular motors operate by repeating cycles, reversible, clean and fatigue-resistant photoreactions are needed. For this reason, only a few types of highly robust and dependable photochemical reactions have been employed so far to operate these systems, namely, photoinduced electron-transfer and photoisomerization processes.[10,20] With regard to the second category, the most

common choice involves photochemical isomerization reactions around (a) C = C (e.g., stilbenes), (b) C = N (e.g., imines), and (c) N = N (e.g., azobenzenes) double bonds.[10,36,37]

A further limitation of light-driven systems is that light absorption phenomena, and so the entire motor operation, are limited by Carnot's efficiency, that is by the difference in temperature between the photon source and the solution.[24,25] Even though this just represents a theoretical limit at this stage, since motors efficiencies are far below the Carnot's limit,[38] it must not be underestimated. In fact, it means that motors operating with photons of lower energy, that is desirable for applications, will be intrinsically less efficient.[24,25]

3.2. Rotary Motors

The vast majority of these molecular motors exhibit controlled unidirectional rotation about a double bond that can be an imine (C=N), or an alkene (C=C).[10,20,36] The double bond photoisomerization is coupled to the thermally activated inversion of planar chirality (thermal helix inversion, THI) that is the main rotation step (Figure 4a). These systems encompass stereogenic elements that break the symmetry of the molecule and of the potential energy surface describing the interconversion between the isomers involved in the operational cycle. Specifically, these molecules must adopt a helical configuration due to the short double bond connecting the sterically demanding aromatic parts of the motor, termed "rotator" and "stator" depending on their moment of inertia.[37,39] The double bond is also the photochromic portion responsible for harvesting the light energy absorbing the photons and bringing the system to higher energy state, generally the first singlet excited state.[40]

Arguably, the most renowned class of light-driven molecular motors is that of *overcrowded alkenes*, where unidirectional rotation occurs about a central C = C double bond.[36] These can be divided into two main classes sharing the alkene motif but with distinct substitution patterns, hence based on different photochromes: the "stilbene" family, where the alkene is flanked by carbon-based aromatic moieties constituting the rotator and the stator (Figure 4b); and the more novel systems based on heterocyclic moieties such as thioindigoid, oxindole, pyrrolidinone, or barbituric acid systems (Figure 4c–f).

Overcrowded stilbene systems bearing at least one point stereogenic element were first reported by Feringa in 1999 and several generations have been developed since then (Figure 4b).[36] Due to the high steric hindrance surrounding the double bond, the molecule is forced to adopt a helical conformation, which chirality is controlled by the configuration at the carbon stereocenter(s). Overall, this class of molecules exists as a mixture of at least four diastereomers thanks to the combination of the point and helical stereogenic elements. They all provide continuous and autonomous 360° rotation about the stilbene C=C double bond under constant light irradiation according to the same flashing energy ratchet mechanism. Absorption of a photon by the stilbene photochrome brings the system into an excited state where the bond order of the alkene is lower, and rotation is allowed. Due to the

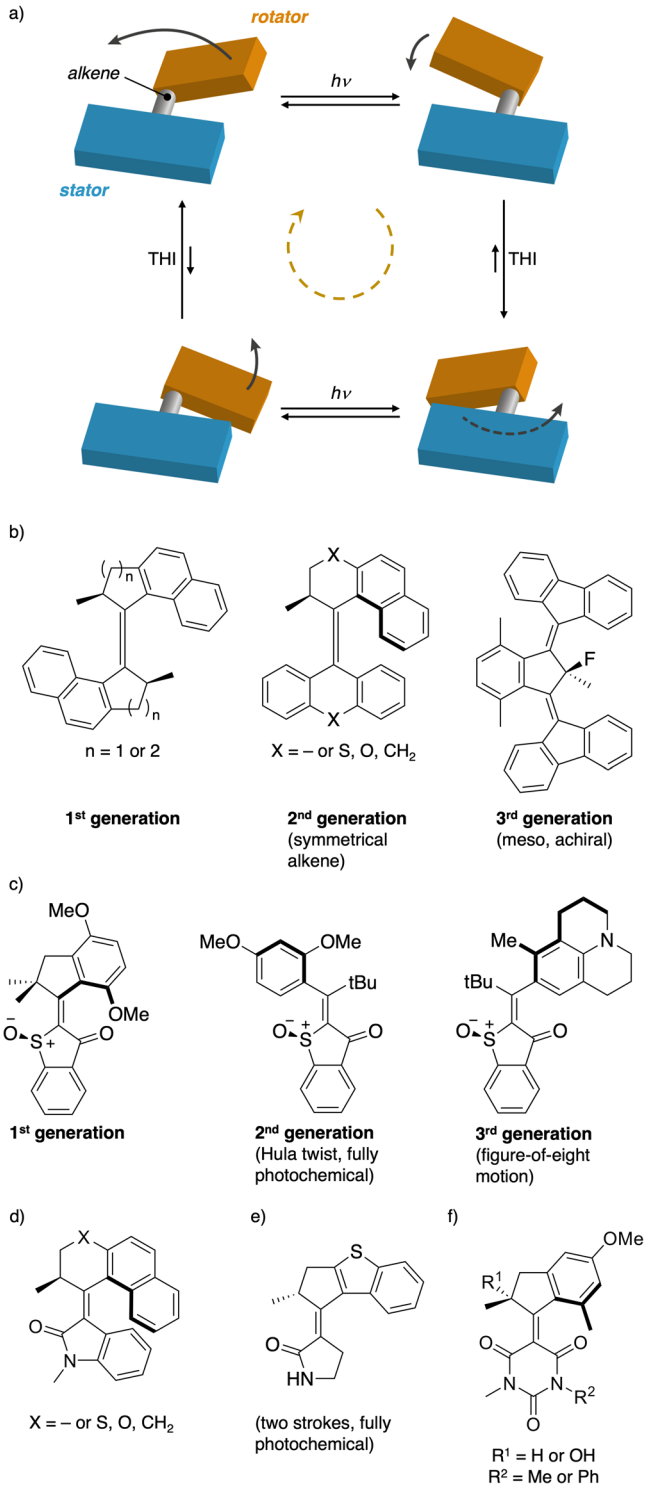

Figure 4. (a) Schematic representation of the four-step closed reaction cycle for the operation of an overcrowded alkene rotary motor. Horizontal processes are photochemical reactions, vertical processes are thermal helix inversions (THI). The black arrows indicate the relative movement of the rotator (orange) with respect to the stator (light blue). The direction of cycling is indicated by the gold dashed arrow. (b) First, second, and third generation Feringa-type motors (ref. [36]). (c) First, second, and third generation hemithioindigo motors (ref. [32]). (d) Oxindole motor class (ref. [57]). (e) Pyrrolidinone two-stroke motor (ref. [31]). (f) Barbituric acid motor class (ref. [62]).

presence of the covalent stereogenic element, the photoisomerization step must proceed via a specific twisted excited state and can, therefore, be directional.[41] Decay to the ground state through conical intersections will generate a photostationary state with a specific composition of the two stable and metastable diastereomers. Aside from the possible *E-Z* isomerism, these isomers differ due to the inverted helicity and the conformation of the methyl group of the stereocenter, which goes from a stable (pseudo)equatorial conformation to a metastable (pseudo)axial conformation. In order to release the strain, the metastable diastereomer undergoes a thermal helix inversion step, which is accompanied by the methyl group relaxation to a (pseudo)equatorial conformation. A second photoisomerization process followed by another THI step close the cycle performing a second 180° rotation in the same direction. THI steps are thermally activated, follow mass action kinetic laws with a specific activation energy barrier related to (pseudo)axial-(pseudo)equatorial conformational change. Given the difference in stability between the two diastereomers the THI step is highly favored thermodynamically and in this case it provides the driving force for motion in the form of a *power stroke*.[10,14,36] This also means that the interconversion from the metastable to the stable diastereomer is responsible for imparting the directionality to the motor. Recently they were able to improve the quantum efficiency and the stability of a second-generation motor by formylation of the aromatic rings. Additionally, the formylation causes a red-shift of the main absorption band, which is beneficial for moving toward operation in the visible light range.[42]

Thanks to their robust and dependable mechanism of operation, this class of motors can perform controlled rotary motion in different environments. For these reasons this type of motors, also known as "Feringa-type motors", were the first to be utilized in prospective applications. The rotary motion has been exploited to increase the topological entanglement in macrocyclic compounds to control a connected property (i.e. a chemical equilibrium constant or a fluorescence quantum yield) or to perform mechanical work on a hydrogel polymer network.[43,44] Additionally, they have been used in biomedical applications as cell culture media, for enhancing diffusion of ions across bilayer membranes, or for disrupting the membrane inducing tumor cell necrosis.[45–47] It should, however, be noted that the role of the motor directionally biased rotation in the latter examples is currently a source of debate.[48]

In their quest to expand the network of reactions to control downstream motion achieving geared motion, the Feringa group, initially reported on a tidal locked motion of a naphthalene moiety around the stator,[49] and more recently they succeeded in coupling the rotary motion with the helicene inversion realizing a controlled paddling motion of the helicene extremities.[50] By a thorough kinetic analysis combined with DFT calculations, the authors could asses that this motor operates through a relatively more elaborated network composed of eight states, six thermal inversion steps coupled to three photoisomerization reactions (Figure 5). In a typical rotation the stable *P-E* isomer undergoes a light induced isomerization of the overcrowded double bond to its *Z* metastable counterpart. The metastable *P-Z*, instead of relaxing via THI to the corresponding stable isomer, inverts the helicene stereochemistry to access the *M-Z* metastable isomer, which then undergoes THI relaxation. In this way the helicene inversion is a direct consequence of the motor switching. A set of analogous transformations alternating photoisomerization, helicene inversion, and THI relaxation, reset the motor to its initial state. The fascinating elaboration of the reaction network brings about significant challenges for its analysis and operational understanding, which highlights the level of sophistication achieved by scientists in studying molecular motors and dissipative systems in general. However, we must note that the reciprocal paddling motion of the helicene would most likely be achieved even if the stilbene portion worked as a simple photoswitch, rather than as a motor displaying unidirectional rotation (lower row in Figure 5).

Since the first reports by Feringa and Lehn on stilbenes and imines respectively in the early 2000s, a plethora of designs emerged, mostly based on heteroatom substituted overcrowded alkenes. These systems have two main advantages, (i) simplifying the synthesis and (ii) reach visible light absorption, which is desirable for future applications.

Fast and efficient directional rotary motion upon visible light irradiation was attained in alkene-based motors by Dube and co-workers upon introduction of a chiral hemithioindigo (HTI) heterocyclic motif at the stator portion.[51] This class of molecular motors proved able to access unconventional pathways for the interconversion of the motor isomers within the closed reaction network such as photon-only operation and hula-twist motion, leading to advanced dynamic features like figure-of-eight trajectories and geared motion through atropisomeric appended arene fragments. Recent reports from the same group address the necessity of innovative experimental and analytical methodologies to access a higher level of insight in the study of ultrafast motors, for which routine techniques present intrinsic limitations. A LED-coupled cryo-HPLC system was developed to overcome the thermal lability and disentangle the individual reactivities of the isomers of a HTI-triptycene photochemical molecular gear.[52] The combination of *in situ* irradiation, stereoisomer separation through a chiral stationary phase and minimized thermal reactions at sub-zero temperatures allowed the isolation of all the isomers composing the closed network and the quantification of inter-isomer photoconversion reactions. Crucially, opposite and nonequivalent directional biases were observed for the *E*- and *Z*- isomers of corresponding configuration, providing the first concrete evidence for a directionally biased molecular gearing process. These results also highlight a more general consideration on the importance of developing novel analytical tools for probing the operation of molecular motors.[53] A complementary experimental strategy was used by the authors to ascertain the directional bias in a fast-rotating HTI motor (Figure 6a).[54] A tetra(ethylene glycol)-triazole tether was used to connect the rotor and atropisomeric stator units into a macrocyclic compound and restrict the accessible rotations to two distinct ~180° clockwise or counterclockwise movements, bound to the configuration of the atropisomeric biaryl fragment and unable to interconvert thermally (Figure 6b). The deter-

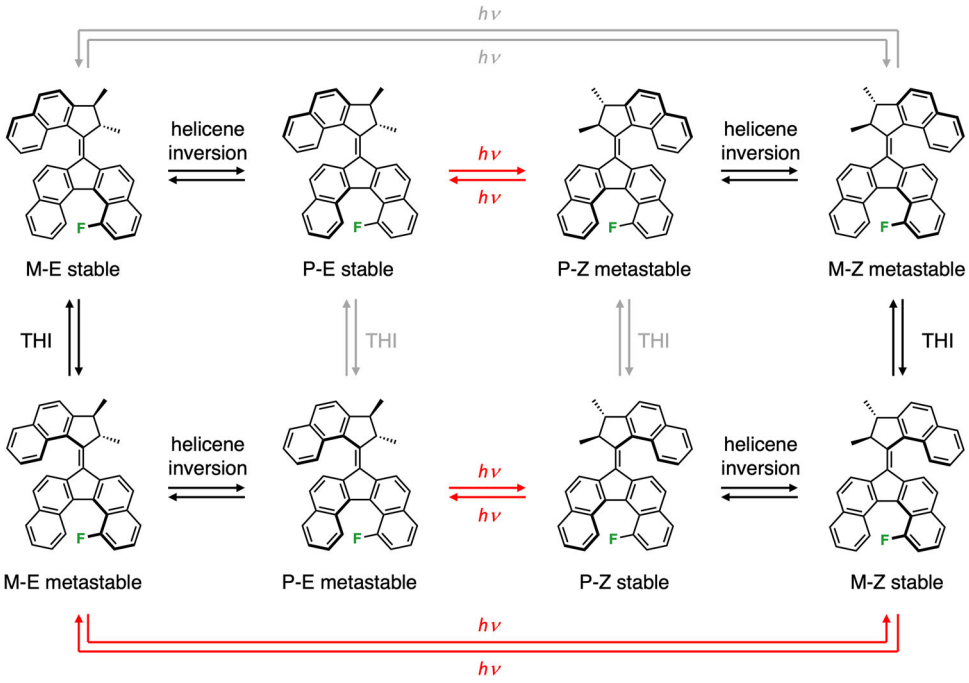

Figure 5. Dual four-step closed reaction cycles that realize the gearing between rotary motion and paddling helicene motion by coupling the photochemical E→Z isomerization reactions (red processes) with helicene helical chirality inversion for the operation of an overcrowded alkene rotary motor (ref. [50]). Thermal inversions (THI and helicene inversion) are indicated in black. The gray arrows indicate processes which proceed at a slower rate compared to all other (photo)chemical reactions. The helical chirality descriptors indicated are relative to the helicene chirality.

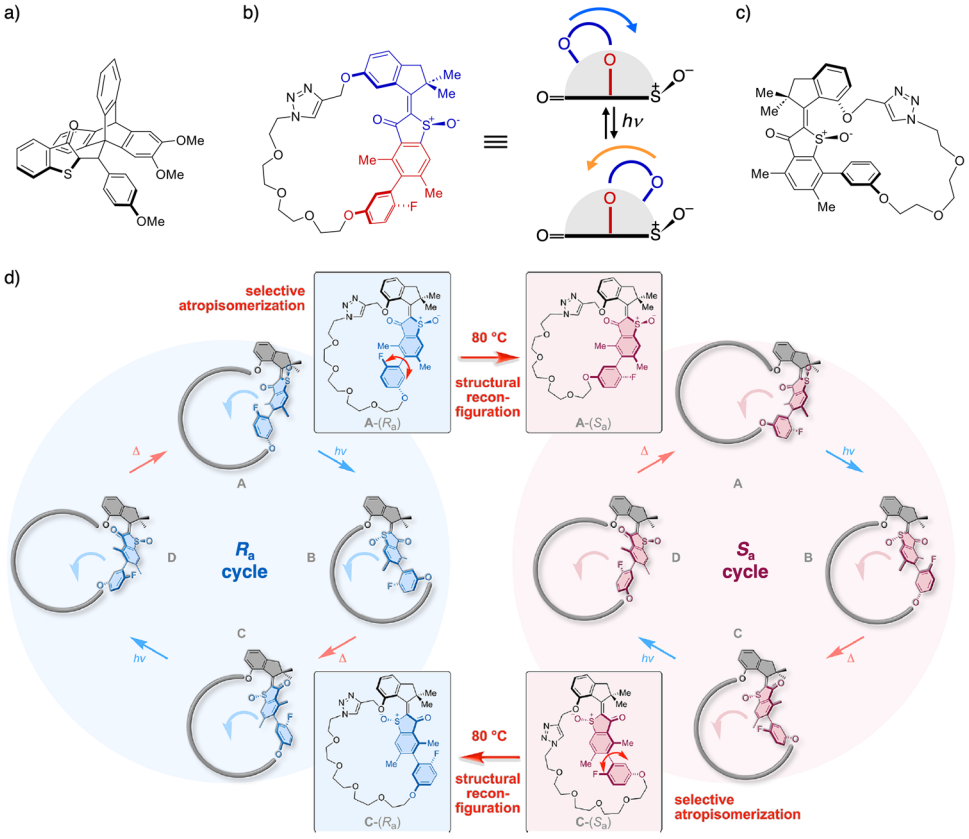

Figure 6. Hemithioindigo based overcrowded alkenes. (a) Triptycene-HTI geared system (ref. [52]). (b) Tether-restricted rotary motion, converting a rotary motor into a switchable system. Adapted with permission from ref. [54]. Copyright 2023, Springer Nature. (c) Structure of the triethyleneglycol restricted motor exhibiting rotation of the tether about a virtual axis. (d) Dual four-step closed reaction cycles interconnected by thermal racemization of an axial chirality element. Adapted with permission from ref. [55]. Copyright 2023, American Chemical Society.

mination of the quantum yields of these two photochemical processes and their comparison to those of the unrestricted HTI motor allowed to discern its preferred directionality. In a recent report, a similar tether-restricted 180° photochemical rotation was coupled to a thermal inversion at the atropisomeric fragment (Figure 6c) to generate a squared closed reaction network.[55] In this case, the directional travel along the closed network translates into a preferential directional spatial movement of the flexible tether about a virtual axis, that proceeds with an opposite direction compared to the corresponding non-tethered motor. The steric constraint inhibiting the rotation is strictly related to the flexibility of the tether, thus extending its length would re-enable a full 360° motion. The authors explored this option by introducing a penta(ethylene glycol) chain in the tether fragment and accessing two diastereomeric macrocycles that differ in the configuration at the atropisomeric biaryl unit (Figure 6d).[56] Importantly, the two reaction cycles identified by these isomers are independently travelled with the same directionality at low temperature due to the high rotational barrier of the biaryl, but become connected at 80°C with a preferential thermal transformation of intermediates **A**-(R_a) →**A**-(S_a) and **C**-(S_a) →**C**-(R_a). Thanks to these selective reconfiguration reactions, an additional level of control on the size and mechanism of travel of the closed reaction network in molecular rotary motors could be achieved.

In 2019, Feringa and coworkers presented a readily accessible version of overcrowded alkene rotary motors featuring an oxindole rotor portion (Figure 4d).[57] The presence of such unit causes a slight red-shift of the absorption bands of the molecular systems, enabling the motors to operate under visible-light irradiation according to the characteristic four-step cycle (Figure 4a). Moreover, the authors demonstrated that the activation energy barrier of the THI could be finely tuned by selecting different rotors (with five- or six-membered rings), thus modulating the rotation rate. Nonetheless, the overall efficiency of these motors is limited by their low quantum yield of photoisomerization which are generally below 3.0 %. To address this limitation, a family of oxindole-based motors was developed that are decorated with electron-donating (i.e. OMe group) or electron-withdrawing (i.e. CN group) substituents in different positions to enhance the charge-transfer character of the systems.[58,59]

This strategy enabled to further red-shift the absorption band in the visible region and increase the quantum yield of photoisomerization up to six-fold compared to the unfunctionalized motors, without altering the THI activation barrier thus affecting the rotation rate. Building on this progress, in 2024 a further improvement of the molecular design of these oxindole-based motors was realized by introducing both electron-donating and electron-withdrawing groups (i.e. OMe and CN groups, respectively).[60] The authors reported that such a rigid push-pull architecture further enhances the photochemical characteristics of the motors, (red-shifted absorption and higher quantum yield of photoisomerization), making them ideal candidates for operation via two-photons absorption. Through this mechanism, they were able to operate this class of rotary motors using near-infrared light.

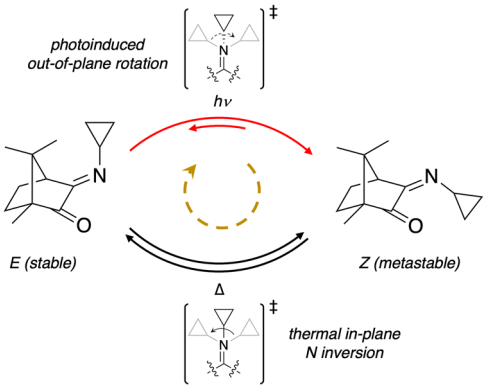

Figure 7. Two-step photothermal operation of Lehn's camphorimine-based motor (ref. [30c]).

A structurally related system was reported by Olivucci and co-workers based on a pyrrolidinone, rather than oxindole, rotator and a benzothiophene containing stator bearing the fixed stereogenic center (Figure 4e).[31] The authors postulated that such overcrowded alkene could operate as a photon-only two-step rotary motor. Although the full 360° unidirectional rotation is only partially supported by experimental evidence, theoretical calculations suggest that the THI steps occur across the excited and the ground states with the common "metastable" helically chiral isomers being in this case transient species not located in a minimum of the potential energy surface. In this way the system converts unidirectionally in a single photochemical step from a stable helical *E* (*Z*) isomer to the corresponding stable *Z* (*E*) isomer.

The possibility to exploit a minimal two-reaction cycle to operate a rotary motor, however, was first demonstrated by Lehn in 2015 combining a photoisomerization with a reciprocal thermal isomerization.[30c] The motor is based on a chiral camphorimine structure in which the photoisomerization of a stable *E* isomer produces a PSS rich in the metastable *Z* isomer (up to 53%) by out-of-plane rotation (Figure 7, red arrows). Interestingly, recent computational studies on a related system showed that the *E*→*Z* photoisomerization proceeds with a directional bias of about 25% thanks to the non-symmetrical energy profile of the excited state.[61] The metastable *Z* isomer then relaxes to the starting–more stable–isomer via a direct in-plane inversion at the nitrogen atom (Figure 7, black arrows). This combination of a photoisomerization and a reciprocal thermal rearrangement is an example of photothermal motor operation (Case 2 in Figure 3c).

In 2023 Crespi and coworkers reported on a readily accessible, visible-light operated class of molecular motors based on an overcrowded alkene flanked by barbituric acid and a 2-methyl-2-hydroxyindane (Figure 4f).[62] This combination provides a photoswitchable system with a push-pull character that features light absorption in the blue visible range, ultrafast isomerization behavior and low THI activation energy. Interestingly, the authors rationalize the lowering of THI energy barrier, as well as that of the thermal *E*→*Z* isomerization, with an intramolecular hydrogen bonding between the hydroxy group of the rotor and the carbonyl moiety of the barbituric acid stator. In fact, the

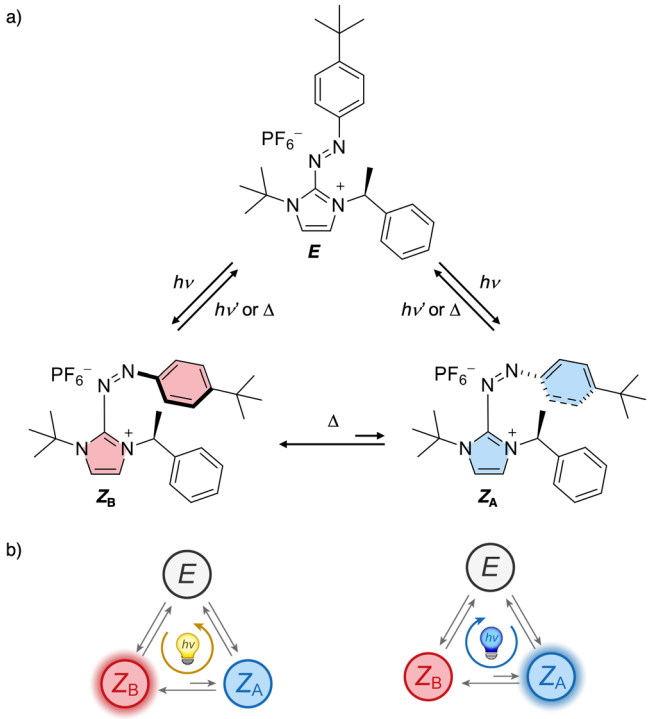

Figure 8. (a) Three-step operating cycle of azoimidazolium rotary motor (ref. [63]). (b) Directionality of travel along the reaction network under irradiation with UV light (left, counterclockwise) or blue light (right, clockwise).

same phenomenon is absent in the corresponding compound lacking the hydroxy group.

Finally, a new class of molecular rotary motors based on an azoheteroarene compound was very recently reported by Curcio and co-workers (Figure 8).[63] This system is composed of a cationic azoimidazolium scaffold in which the azolium heterocycle bears two different substituents, one carrying a fixed stereogenic center. Irradiation with consequent *E*→*Z* isomerization of the diazene unit generates two diastereomeric *Z*-species endowed with axial chirality that dynamically interconvert through a thermal rotation about a single C—N bond. This epimerization equilibrium together with the (photo)conversion with the parent *E*-species, which lacks the axial chirality element, define a triangular closed reaction network (Figure 8a). The different stability of the *Z* diastereomers enables, under constant irradiation, net directional travel along the closed network. Remarkably, the preferential direction adopted by the system is highly dependent on the wavelength of the light used and inverts upon switching from UV (365 nm, Figure 8b, left) to visible light (453 nm, Figure 8b, right), feature common in biological rotary motors and yet unreported for artificial ones.

3.3. Linear Motors (Pumps)

Pioneering work on the light-fueled linear translocation of rings along an axle was done by the groups of Leigh, who reported the first experimental realization of a Maxwell's demon in 2007,[64] and by Stoddart and coworkers who operated an

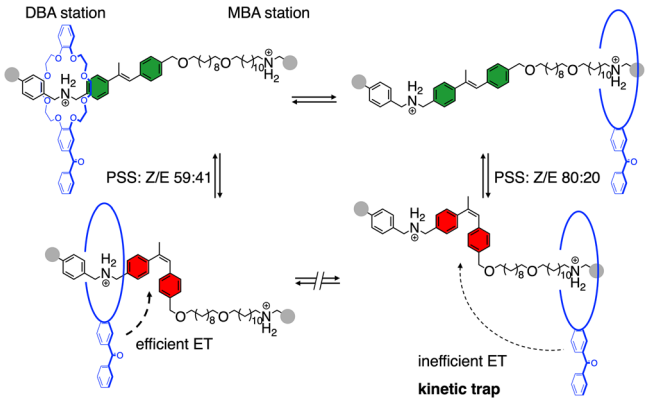

Figure 9. Four-step reaction cycle operating a light-driven information ratchet (Maxwell's demon, ref. [64]). The dashed arrows represent energy transfer from the macrocycle to the stilbene "gate". The thickness of the arrow indicates the efficiency of energy transfer which is reflected in a different PSS for the two mechanical isomers. The crown ether is schematized as a ring in the top right and bottom structures. Filled gray circles represent stoppering units.

electrochemically-fueled linear supramolecular pump using photoinduced electron transfer in 2013.[65] In particular, the Leigh group designed the first photochemical information ratchet based on a [2]rotaxane architecture. The system encompasses a dibenzo[24]crown-8-ether ring equipped with a benzophenone photosensitizer that can shuttle between two ammonium stations slipping over a stilbene moiety. The ring shuttling motion is free when the stilbene is in the *E* configuration, whereas the *Z*-stilbene acts as a stopper (Figure 9). Irradiating the system, in presence of benzil as the photosensitizer, the stilbene gate reaches a PSS rich in *Z* (*Z*/*E* 80:20), preventing the ring shuttling motion. Initially, the relative population of macrocycles on the dibenzylammonium station (DBA) is 65%, essentially identical to the value in the dark (equilibrium). Thanks to the asymmetric position of the stilbene gate along the axle, however, efficient energy transfer (ET) from the ring-bound benzophenone to the stilbene can occur when the macrocycles is on the DBA station. This brings the PSS of this mechanical isomer to 59:41 (*Z*/*E*) and rings can shuttle toward the monobenzylammonium station (MBA). Conversely, energy transfer from macrocycles on the MBA station is not efficient. The stilbene gate, thus, reverts back to the *Z*-rich PSS preventing macrocycles to re-equilibrate between the two stations. In this way, under continuous irradiation, macrocycles are kinetically trapped on the MBA station realizing a non-equilibrium distribution of the two mechanical isomers with the relative population on the DBA station reduced to 45%. Effectively, the system continuously consumes light energy to sustain a non-equilibrium distribution of the mechanical isomers. The system operates according to an information ratchet mechanism due to the different rates of the *E*→*Z* and *Z*→*E* photoconversion for the two mechanical states (Case 3, photochemical gating in Figure 3d). This is realized by linking the quantum yields of photoisomerization and the molar absorption coefficients of the stilbene to the ring position along the axle.

The first autonomous system that combines directly continuous, non-reciprocating, linear ring sliding with light energy

consumption, realizing a linear motor fueled by light, was reported by Credi and coworkers. In 2015 they introduced a supramolecular pump (linear molecular motor) autonomously converting light into chemical energy through an energy ratchet mechanism.[66] Over the last 5 years, the authors developed a family of compounds all based on a similar architecture characterized by an asymmetric axle equipped with a central ammonium station flanked by a photoactive azobenzene chromophore and a non-photoactive "pseudostopper" (Figure 10a,b).[67] From a reactions network point of view, the system is analogous to the covalent rotary motors with the photochemical processes directly coupled to the thermal reactions (Figure 10a). In the dark, the supramolecular complex between the ammonium and the crown ether forms via slippage over the azobenzene moiety. Upon light irradiation the isomerization of the azobenzene moiety occurs, which brings about two main consequences: (i) the increase of the slippage barrier to a level higher than that of pseudostopper, and (ii) the destabilization of the supramolecular interactions between the crown ether and the ammonium group ($K_Z < K_E$, power stroke). The consequence is that rings will leave the axle slipping over the pseudostopper. The directionality of the slippage processes is ensured by the appropriate choice of pseudostopper, with a kinetic barrier for slippage falling in between that of the *E* and *Z* azobenzene (Figure 10b). The autonomous operation of this linear motor is achieved thanks to the overlapping absorption bands of the azobenzene photochrome which ensures that photons of the same, appropriate, wavelength can trigger both $E \rightarrow Z$ and $Z \rightarrow E$ photoisomerization, thus powering the energy ratchet. Therefore, under constant light irradiation, the supramolecular complex between the axle and a crown ether macrocycle, formed by slippage of the crown ether over the axle, undergoes continuous and autonomous dissipative self-assembly. The macroscopic result, that is, the kinetic trapping of a metastable species driven to relax, is basically identical to the one observed in Leigh's stoppered system. However, differences emerge from a molecular perspective. In Credi's system energy consumption is associated with the continuous, directionally biased, ring slippage over the axle (i.e. pumping): the single macrocycle is first trapped in a high energy complex and then released in solution to restart the cycle.[68] On the other hand, in Leigh's system a single ring is trapped in a high energy state but the pumping cycle is not realized. In 2022 the same authors characterized the pump's dissipative operation by means of a combined experimental and theoretical approach, elucidating the dependance of several parameters of operation on the photon flow.[38] The picture that emerged was that rate of operation, and thus the amount of energy that can be stored and dissipated by the system increase to an upper limit (Figure 10c). More importantly, the steady state efficiency of the system decreases at higher photon flow, both in terms of energy transduction efficiency, Carnot-type efficiency and quantum efficiency (Figure 10d). This finding was explained with the switching from a photochemically limited kinetic regime to one characterized by rate limiting self-assembly steps, which cannot cope with the fast photochemical processes. The result is that more energy is dissipated by the photoisomerization steps. The importance of this contribution lies in its broad applicability to light-fueled systems. In fact, several of the limiting factors highlighted in this study can be generalized to other light-fueled motors and the theoretical framework applied allows the quantitative comparison of light-operated molecular motors with their electrochemically- and chemically-driven counterparts. Finally, for the first time this work connects the operation of a light-fueled motor with the Carnot's efficiency of a corresponding thermal machine, in a certain way closing a gap between nano- and macroscopic machines.

Combining pH variations and light irradiation, the same authors developed a doubly responsive rotaxane linear molecular motor (Figure 10e).[69] Early examples of a similar light-driven autonomous reciprocating motion were the, already discussed, Maxwell's demon[64] and the 2006 autonomous "four-strokes motor" by Balzani and Stoddart.[21] There, photoinduced electron transfer was exploited to continuously drive the distribution of crown ether rings in a [2]rotaxane from a stable viologen station to a higher energy 4,4'-dimethyl viologen station.

In this new example, the combination of two possible states generated by each input (protonated/deprotonated and *E*/*Z*) allowed the definition of a square network of chemical and photochemical reactions that can be travelled directionally through a careful interplay between the specific acidity and thermal reactivity of its constituting isomers. More specifically, when simultaneously present in solution, the most acidic compound *Z*-protonated can react with the most basic compound *E*-deprotonated (Figure 10e, central black dashed arrows) to form the *Z*-deprotonated isomer. This species has a rate of thermal back isomerization 17 times faster compared to that of the *Z*-protonated species and siphons away *Z* species. Combining the intrinsic directionality of the two processes, in the presence of a sub-stoichiometric amount of protons and under continuous light irradiation the network is travelled preferentially in a counterclockwise direction.

4. Chemically-Fueled Molecular Motors

One of the main advantages of using chemical energy, lies in the readiness of employment and in the fast response timescale. The main limitation to the rate of operation of the motor is the rate at which the fuel is converted to waste.[9a,70,71] It is not a surprise, after all, that most bacteria and all animals use chemical fuels—e.g., ATP—to power their systems, due to the necessity of fast response to environmental changes and sustaining increasingly complex systems (e.g., nervous systems).[71]

4.1. Operating Principles

This class of motors harvests the chemical potential of a selected "fueling" reaction to ratchet the Brownian motion of the isomerization (mechanical) process. In order to operate autonomously, the cycle of transformations (Figure 11a) must involve (i) the interconversion between distinct isomers (mechanical motion, reactions *1* and *3* in Figure 11a); (ii) the fuel consumption mediated by each isomer (energy harvesting, reactions *2* and *4* in

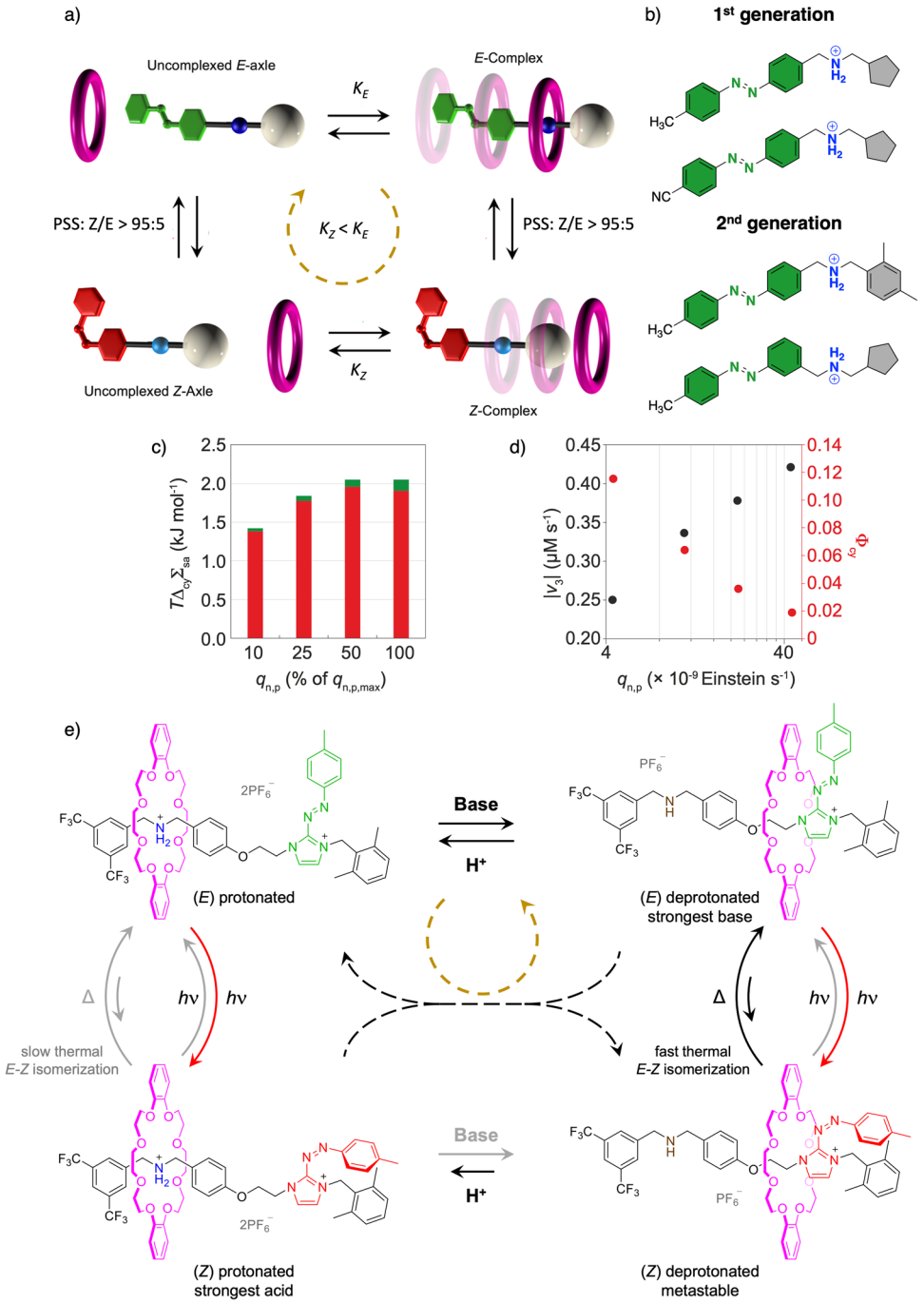

Figure 10. (a) Schematic representation of the four-step reaction network describing the operation of Credi's supramolecular pump (ref. [66]). The network includes two photochemical (vertical) and two self-assembly (horizontal) reactions. (b) First- and second-generation supramolecular pumps non-symmetric axles (ref. [67]). (c) Energy dissipated by the self-assembly steps for E (green bars) and Z (red bars) configurations and (d) cycling rate (black dots) and quantum yield (red dots) values at different light intensities. Adapted with permission from ref. [38]. Copyright 2022, Springer Nature. (e) Closed reaction network describing the operation of Credi's linear motor driven by allosteric photoregulation of amine basicity with internal proton exchange (black dashed arrows, ref. [69]). The gray arrows indicate processes which proceed at a slower rate compared to all other (photo)chemical reactions. The dashed gold arrows in (a) and (b) indicate the directionality of network travelling under dissipative operation.

Figure 11a); finally, (iii) to reset the system, close the cycle, and render the motor autonomous, a second set of reactions is needed to bring about an opposite transformation than the fuel consumption, generating a stoichiometric amount of waste (reactions *2′* and *4′* in Figure 11a). These reciprocal transformations must be able to occur simultaneously under the same experimental conditions, yet they must be different from the microscopic reverse of the fueling reaction.[71] Effectively, a chemically-fueled motor must be a catalyst for mediating the fueling reaction with distinct kinetics for each "mechanical" isomer in order to break detailed balance and install kinetic asymmetry in the reaction cycle (Equation 3 and Figure 11b).[70]

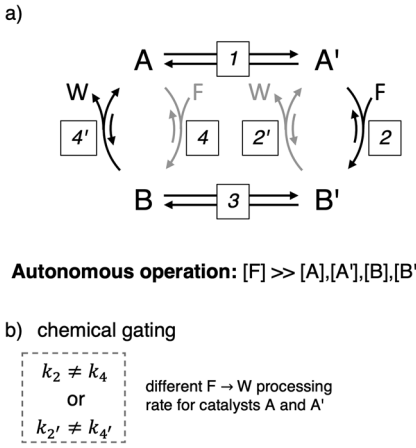

Figure 11. (a) Minimal reaction network for realizing an information ratchet for the autonomous operation of a chemically fueled molecular motor. The labels "F" and "W" stands for "fuel" and "waste" respectively. (b) The fuel processing and the reciprocal waste formation steps proceed at different rates based on the catalyst isomer (A/B or A′/B′, chemical gating). To highlight the kinetic asymmetry, reactions that proceed at a slower rate than their counterparts in the other mechanical isomer are represented by grey arrows.

$$K_r = \frac{k_1}{k_{-1}} \times \frac{k_2\,[F] + k_{2'}\,[W]}{k_{-2} + k_{-2'}} \times \frac{k_{-3}}{k_3} \times \frac{k_{-4} + k_{-4'}}{k_4\,[F] + k_{4'}\,[W]} \quad (3)$$

In this way, what is realized is a kinetic gating of the two reciprocal steps which ensures autonomous operation reaching a steady state.[71,72] This mechanism of operation, being solely based on kinetic considerations of the processes involved, means that chemically-fueled motors, unlike macroscopic heat engines and light-operated systems, are not subjected to Carnot's theorem and could, in principle, approach perfect efficiency.[71,73] Additionally, since all chemically-fueled motors are essentially information ratchets, the presence of a *power stroke* is not a prerequisite.[14,17,74–76]

By comparing Equations (2) and (3) it emerges that the photochemical gating in light-fueled motors (Figure 3d), is analogous to the chemical gating and represents essentially the same information ratchet scheme despite the different intrinsic physical mechanisms. In both cases, in fact, the kinetic asymmetry is related to the differences in the kinetics of fuel processing, expressed by the second and fourth terms of both equations. In the case of light-fueling these terms are described by photoconversion parameters: quantum yields, molar absorptivities, and the photokinetic factor.[24,38] Conversely, for the chemically-fueled systems they include the rate constants of the fuel-to-waste conversion catalytic cycles and the concentrations of fuel and waste.

In principle, any exergonic reaction can be exploited to run a motor and any catalytic cycle could be repurposed to become a motor.[72,77] On a practical level, though, much less options are available, due to the fundamental aspect of having two reciprocal reactions operating simultaneously, and to the need for catalytic fuel decomposition mediated by the motor. Nature uses catalytic ATP hydrolysis and the reciprocal reactions are the *on* and *off* rates of the enzyme motor in the distinct conformations.[13,78] However, this strategy requires a very high level of sophistication of the catalytic active site.[79] So far, artificial systems have exploited ester, carbamate, anhydride formations driven by activated esters or carbodiimides and the subsequent product hydrolysis.[77,80] These are bimolecular reactions, therefore their relative kinetic can be tuned by changing the reagents concentration to reach a state where they can occur simultaneously at comparable rates.

4.2. Rotary Motors

The first idea of preparing a small molecule capable of rotating in a preferential direction about a single covalent bond when subjected to chemical stimuli was developed by Kelly in the 1990s. Even though they never succeeded in realizing a full 360° relative rotation of the rotor and stator residues, these examples were the first experimental realization of the nanoscopic ratchet and pawl theorized by Feynman in the 1960s and represent the cornerstone for all future developments.[12,81] We had to wait until 2016 for the first successful realization of an autonomous, chemically fueled molecular motor by the Leigh group.[82] This motor is based on a [2]catenane architecture where a small ring can shuttle between two distinct fumaramide stations located on le the larger ring track (Figure 12a). The stations are separated by alcohol moieties protected by 9-fluorenylmethoxycarbonyl (Fmoc) groups. During operation, the Fmoc groups are continuously hydrolyzed thanks to the presence of a base in solution and substituted by new Fmoc groups thanks to the presence of Fmoc chloride (Fmoc-Cl) and a pyridine-based catalyst. Effectively Fmoc-Cl is consumed by the motor to rotate preferentially in one direction and serves, thus, as the fuel. The operational principles rely on the different rates at which all these processes occur with respect to the distance of the ring from the reactive alcohol/Fmoc. Specifically, the Fmoc deprotection rate is almost independent from ring position. Conversely, the nucleophilic attack of the hydroxy group to the Fmoc-Cl fuel occurs at a faster rate when the ring is far and is slower when the ring is in its proximity. Effectively, the free hydroxy moiety serves as a catalyst for the conversion of Fmoc-Cl in CO_2 and dibenzofulvene. This kinetic gating is at the core of the "information ratchet" mechanism that drives the motor unidirectionally, since the rate constant of the fueling chemical reaction depends on the position of the Brownian particle—that is, the small ring. Overall, the small ring moves along the circular track by Brownian motion and the OH groups, that are transient under reaction conditions, are derivatized biasing its position. The concurrent Fmoc derivatization and hydrolysis (reciprocal reactions) ensure autonomous operation.

Thanks to its relatively simplistic design and straightforward operation compared to the natural counterparts, this motor represented one of the first benchmarks for testing theoretical modelling,[83] novel thermodynamic approaches,[84] and, more generally, our understanding of the operation of non-equilibrium chemically-fueled systems.[74] Penocchio and Leigh reported on an information thermodynamic analysis of the sys-

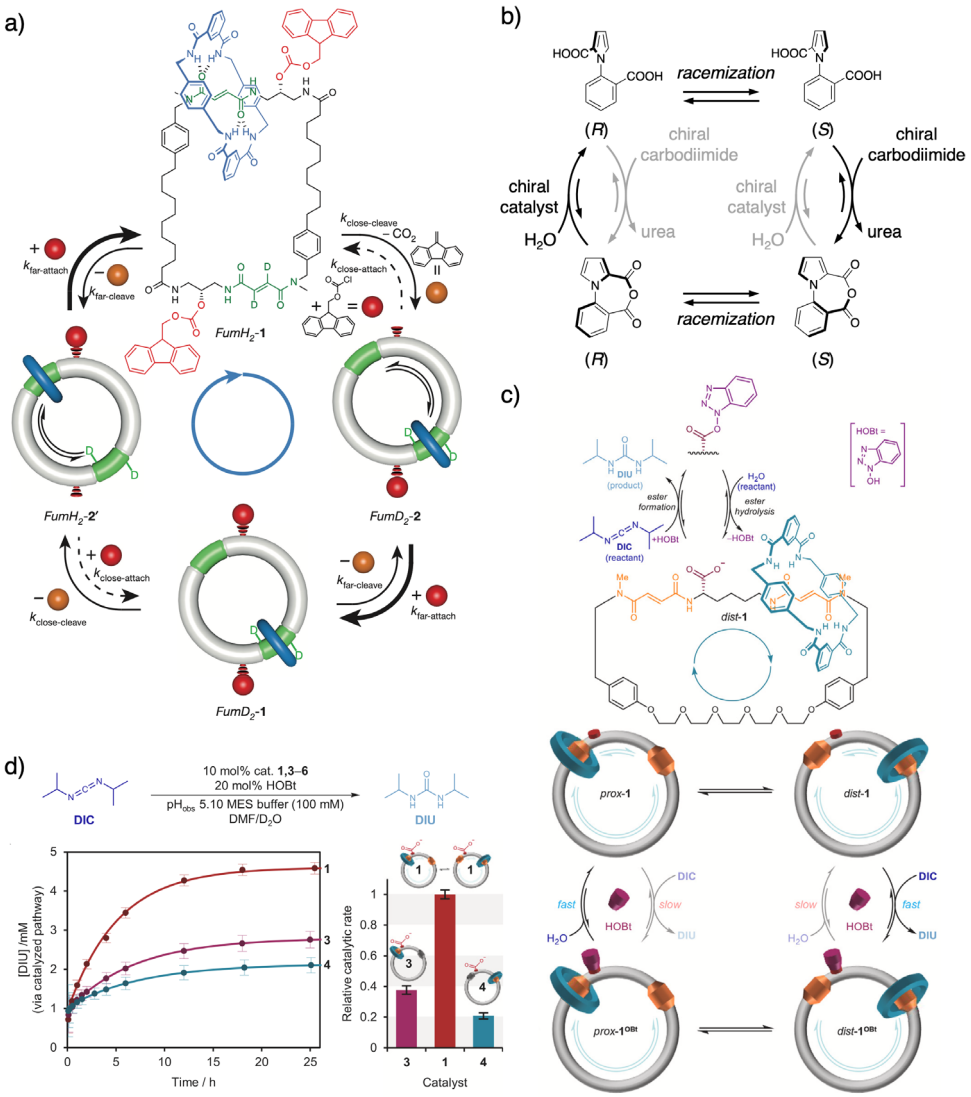

Figure 12. (a) Schematic mechanism of operation of the first chemically fueled catenane rotary motor based on an information ratchet. The double arrows do not represent chemical equilibria but the two reciprocal processes of Fmoc derivatization and hydrolysis. Reproduced with permission from ref. [82]. Copyright 2016, Springer Nature. (b) First small molecule rotary motor based on an information ratchet (ref. [86]). Gray arrows represent kinetically slow processes. (c) Rotary motor dynamic catalyst for hydrolysis of diisopropylcarbodiimide and (d) kinetic traces for the hydrolysis reaction and relative catalytic rate comparing the (co)conformationally dynamic catalyst (red trace and bar) and the corresponding dynamically impaired control compounds (purple and blue traces and bars). Adapted with permission from ref. [89]. Copyright 2024, Elsevier.

tem that revealed the purely kinetic basis of operation of the motor. The same study also provides insights in the role of power stroke in a pure information ratchet, like this motor, to tune rotation rate and operation efficiency.[84]

After introducing the use of carbodiimides to fuel molecular ratchets and motors,[85] the Leigh group also reported on a non-interlocked small molecule that operates as a chemically fueled motor. The design is based on a substituted N-phenylpyrrole that can rotate unidirectionally about the C—N single bond through a four-step network (Figure 12b).[86] The scaffold is substituted with two carboxylic acid moieties in 2 and 2′. Thanks to this substitution pattern the C-N bond exhibit planar chirality and the molecule exists in two atropisomers that are in chemical exchange at room temperature. Importantly, though, interconversion occurs only with the carboxylic acid passing over the small substituent. In presence of a chiral carbodiimide, the two carboxylic acids react to form an anhydride preferentially via one atropisomer, that is forcing the scaffold to rotate in a preferred direction about the C—N bond. Analogously to the diacid, the anhydride can also interconvert between two atropisomers, however, since the carboxylic acids are linked together, interconversion must occur by inversion of the seven membered ring puckering. The use of a chiral catalyst to hydrolyze preferentially one enantiomer of the anhydride induces a second 180° rotation about the C—N. Overall, matching the chirality of the fuel (carbodiimide) and of the hydrolysis catalyst can result in a 360° rotation with net directionality. Effectively, the described approach is basically the combination of two dynamic kinetic resolution steps for both the reciprocal processes that drive the motor.[84] It is worth noting that the direction of rotation of the

motor is not controlled by a chiral element of the motor itself, but by the chirality of the fuel/catalyst. The same motor can, thus, rotate both clockwise and counterclockwise. Additionally, in the absence of a power stroke, the ratcheting constant must be related directly to the enantioselectivity of the resolution steps, in fact the directional bias of the reported system is about 70%. It is therefore possible to achieve nearly perfect unidirectionality by optimizing the enantioselectivity of the reciprocal processes. These are intrinsic characteristic of chemically fueled motors which stems directly from the all-thermal mechanism of operation. Leigh and Giuseppone very recently introduced this motor as a crosslinker within an hydrogel matrix to induce macroscopic expansion and contraction of the gel fueled by a chemical species.[87] Interestingly, this approach allows to both shrink and relax the gel since the direction of rotation is related to the chirality of the fuel. In a related report, the authors also elaborated on the importance of the chemical fuel structure for the ratcheting performance. The structural features of the fuel markedly influence the energy storage, cycle directionality and rate of operation due to the secondary interactions between the fuel and the ratchet.[88]

As mentioned in the previous section, this class of molecular motors operate by catalyzing the conversion of a chemical fuel into waste to harness the ΔG of reaction and rectify the Brownian motion. In 2024, Leigh demonstrated that catalyzing a reaction through a molecular motor opens intriguing insights in how the (co)conformational dynamics of the motor/catalysts affects the reaction rate.[89] They exploited a two-station catenane to catalyze the hydrolysis of diisopropylcarbodiimide (DIC) to diisopropylurea (DIU), through a benzotriazole ester intermediate. The benzotriazole then undergoes uncatalyzed hydrolysis to reform the active catenane catalyst (Figure 12c). Formation of the HOBt catenane intermediate occurs faster when the ring is away from the nucleophilic hydroxy group, whereas hydrolysis is faster when the ring is close to the HOBt ester thanks to hydrogen bond coordination to the ester group. Since (co)conformational isomerization is always allowed thanks to the catenane architecture, both transition states can be accelerated by the distinct coconformers, resulting in a faster carbodiimide hydrolysis compared to (co)conformationally locked systems (Figure 12d). Incidentally, the small ring must circulate around the larger ring with a directional bias due to the reciprocal reactions and the catalytic mechanism of operation. Potentially, these results pave the way for understanding why Nature often uses motors to catalyze reactions and designing artificial systems that exceed intrinsic catalytic limitations, such as the Sabatier's limit.

4.3. Linear Motors (Pumps)

Basing, again, on Fmoc derivatization and cleavage as reciprocal reactions, the Leigh group also reported on a linear motor for accumulating on an axle molecular ring free floating in solution—that is, a chemically fueled pump.[90] The pump is based on a ring catching oligotriazole chain stoppered on one side and with a reactive benzylamine on the other. The system is also equipped with a trifluoromethyl pseudostopper close to the reactive site (Figure 13a). The operation mechanism is based on the crown-ether active templated formation of an Fmoc carbamate at the benzyl amine site.[91] The weak complex between the 24-crown-8 ether ring and the primary benzylamine promotes the reaction with the Fmoc p-nitrophenyl ester (Fmoc-OPNP), effectively gating the kinetics of Fmoc amine derivatization and trapping the ring around the axle. The carbamate formed upon active templated synthesis represents a weak station for the crown ether ring, which shuttles toward one of the triazole stations on the ring catching chain after slipping over a trifluoromethyl group which serves as a "speed bump" slowing down the rings release when the Fmoc stoppering group in not present. Under operation, the Fmoc carbamate is continuously hydrolyzed by diisopropylamine present in solution and the amine restored for another pumping cycle. The catalytic active templated Fmoc stoppering is at the basis of the information ratchet mechanism of operation and this pump is capable to trap up to three rings per collecting chain at the expenses of a chemical fuel (Fmoc-OPNP). Interestingly, the Fmoc removal was found to be slower when rings are on the thread indicating that the reciprocal hydrolysis reaction is also kinetically gated in this system. This is, most likely, due to the ring encircling the carbamate station is affecting the kinetics of the Fmoc deprotonation step. Such a double kinetic gating helps the operation by stabilizing the pumped rotaxanes and depleting more efficiently the stoppered free axles, formed by uncatalyzed benzylamine Fmoc-OPNP reaction, which become more readily available for pumping. Additionally, it is worth noting that ring translocation between the carbamate to the triazole station ((co)conformational isomerization) plays the role of a power stroke in this information ratchet system.

Later, the same group also demonstrated the possibility of using a similar approach to synthesize "impossible"—that is, without recognition motifs between rings and axles—[n]rotaxanes ($n > 2$) via a stepwise pumping and transamidation stoppering strategy (Figure 13b).[92] The crown ether active templated amide formation is exploited to trap the ring on the axle where the formed amide acts as a weak station (pumping step). Subsequently, the amide nitrogen is derivatized with a *t*-butyloxycarbonyl (Boc) protecting group, forming an N-carboxylated intermediate and forcing the ring to shuttle onto the oligoethylene glycol chain (shuttling step). After converting the N-carboxylated amide into a bromophenolic active ester, using a bulky 2,6-dimethyl-4-bromophenol to prevent rotaxane disassembly (activation step), another active templated amide formation step can be performed to trap a second ring. This cycle, that implements a stepwise information ratchet mechanism, can be repeated and up to four crown ether macrocycles can be trapped on the axle by consuming the benzylamine. This strategy also allows to control the sequence isomerism of the formed rotaxanes by pumping different macrocycles at each transamidation cycle.

5. Conclusions and Future Perspectives

This review detailed the latest advancements in the field of autonomous molecular motors, highlighting the common

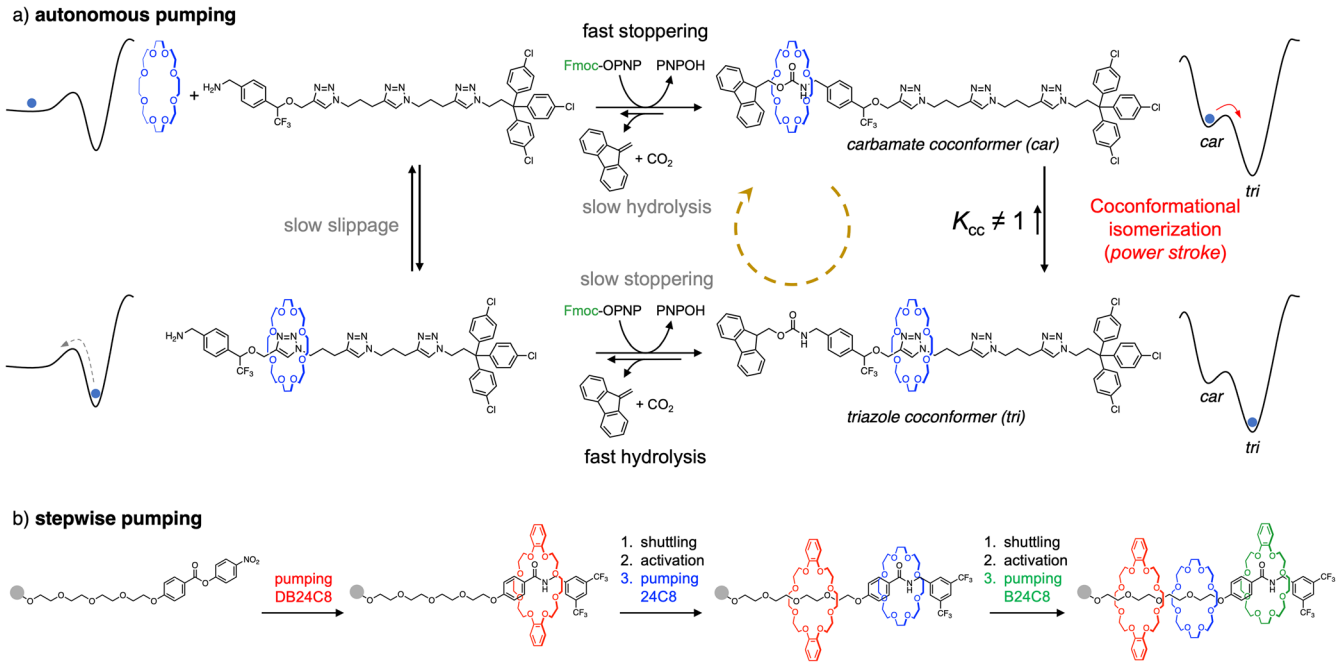

Figure 13. (a) Simplified kinetically gated reaction network for pumping one 24-crown-8 onto the axle (ref. [90]). The pump undergoes multiple cycles following an analogous scheme to pump three macrocycles, since the slippage from the unstoppered axle is slower than the stoppering reaction. Slow processes are indicated in gray, the dashed gold arrow indicates the directionality of the network under dissipative operation. (b) Stepwise crown ether pumping to produce a sequence-specific [4]rotaxane (ref. [92]). Filled gray circles represent stoppering units.

ground behind their successful operation. We envisage that, by taking advantage of their individual characteristic features, in the near future both light- and chemically-fueled systems will express their full potential by bringing about groundbreaking innovations in particular within the field of bio-nanotechnology. Advanced systems that operate autonomously will play a pivotal role in the development of artificial living cells, to sustain fundamental life-like tasks (e.g., transport, growth and replication). Toward this goal, essential requirements for their development include: (i) accessing structures and (photo)reactivities compatible with aqueous environments to implement effective motor operation in water and compartmentalized systems (i.e. bilayer membranes, liposome lumen) and (ii) taking full advantage of the controlled unidirectional motion of molecular motors to enable motility across distances longer than their size. Although seminal work has been done in these directions,[44,93–95] the potential of controlled nanoscale motion has yet to be fully exploited.

Pumping entities across membranes is currently almost exclusively limited to ions and mostly using systems that do not require the directional motion of their subunits.[93,94] Conversely, exploiting long-range motion rectification could enable the development of molecular pumps with a wider scope of pumped substrates (e.g., molecules, oligomers, bioactive fragments).

Strategies to amplify the directional motion across length scales are still in their infancy, with reported examples mostly focusing on geared motion of (sub)molecular fragments, eventually embedded within soft materials.[44,49,50,51] Advances in this field would have the potential for the development of macroscopic kinematic chains toward active motility (e.g., artificial flagella, chemotaxis and phototaxis) and responsive materials of high applicative potential (e.g., acrylates, thermosets).

The attainment of these goals, along with the implementation of life-compatible (photo)chemical reactions will also allow to interface the next generation of artificial systems with natural ones, potentially avoiding any interferences with the myriad of processes simultaneously occurring in the cell.

Acknowledgements

The authors are thankful to Dr. Emanuele Penocchio for proofreading the manuscript and providing valuable insights. Financial support from the European Union through NextGeneration EU–Mission 4, Component 2, Investment 1.1 (PRIN 2022 project "Embrace" 2022KMMAYM, CUP J53D23008720006) is gratefully acknowledged.

Open access publishing facilitated by Universita degli Studi di Bologna, as part of the Wiley - CRUI-CARE agreement.

Conflict of Interests

The authors declare no conflict of interest.

Keywords: Autonomous operation · Catalysis · Dissipative systems · Molecular motors · Photochemistry

[1] a) D. S. Goodsell, *The Machinery of Life*, Copernicus, **2009**; b) M. Schliwa, G. Woehlke, *Nature* **2003**, *422*, 759–765.

[2] a) N. J. Carter, R. A. Cross, *Nature* **2005**, *435*, 308–312; b) U. Hübscher, G. Maga, S. Spadari, *Annu. Rev. Biochem.* **2002**, *71*, 133–163; c) B. J. Foth, M. C. Goedecke, D. Soldati, *Proc. Natl. Acad. Sci. USA* **2006**, *103*, 3681–3686; d) N. Hirokawa, Y. Noda, Y. Tanaka, S. Niwa, *Nat. Rev. Mol. Cell Biol.* **2009**, *10*, 682–696; e) T. Minamino, K. Imada, *Trends Microbiol.* **2015**, *23*, 267–274.
[3] C. von Ballmoos, G. M. Cook, P. Dimroth, *Rev. Biophys.* **2008**, *37*, 43–64.
[4] P. Ernst, D. T. Lodowski, M. Elstner, P. Hegemann, L. S. Brown, H. Kandori, *Chem. Rev.* **2014**, *114*, 126–163.
[5] The definition of "spectral radiant power" is in accordance with, J. W. Verhoeven, *Pure Appl. Chem.* **1996**, *68*, 2223–2286.
[6] a) E. Schrödinger, *What is Life? The Physical Aspect of the Living Cell*, Cambridge University Press, Cambridge, UK **1944**; b) S. Ornes, *Proc. Natl. Acad. Sci. USA* **2017**, *114*, 423–424.
[7] L. Zhang, Y. Qiu, W.-G. Liu, H. Chen, D. Shen, B. Song, K. Cai, H. Wu, Y. Jiao, Y. Feng, J. S. W. Seale, C. Pezzato, J. Tian, Y. Tan, X.-Y. Chen, Q.-H. Guo, C. L. Stern, D. Philp, R. D. Astumian, W. A. Goddard III, J. F. Stoddart, *Nature* **2023**, *613*, 280–286.
[8] a) H. L. Tierney, C. J. Murphy, A. D. Jewell, A. E. Baber, E. V. Iski, H. Y. Khodaverdian, A. F. McGuire, N. Klebanov, E. C. H. Sykes, *Nat. Nanotechnol.* **2011**, *6*, 625–629; b) T. Kudernac, N. Ruangsupapichat, M. Parschau, B. Maciá, N. Katsonis, S. R. Harutyunyan, K.-H. Ernst, B. L. Feringa, *Nature* **2011**, *479*, 208–211; c) G. J. Simpson, M. Persson, L. Grill, *Nature* **2023**, *621*, 82–86
[9] a) K. Das, L. Gabrielli, L. J. Prins, *Angew. Chem., Int. Ed.* **2021**, *60*, 20120–20143; b) D. Del Giudice, S. Di Stefano, *Acc. Chem. Res.* **2023**, *56*, 889–899.
[10] a) S. Kassem, T. van Leeuwen, A. S. Lubbe, M. R. Wilson, B. L. Feringa, D. A. Leigh, *Chem. Soc. Rev.* **2017**, *46*, 2592–2621; b) M. Baroncini, S. Silvi, A. Credi, *Chem. Rev.* **2020**, *120*, 200–268.
[11] a) D. Dattler, G. Fuks, J. Heiser, E. Moulin, A. Perrot, X. Yao, N. Giuseppone, *Chem. Rev.* **2020**, *120*, 310–433; b) V. García-López, D. Liu, J. M. Tour *Chem. Rev.* **2020**, *120*, 79–12.
[12] D. J. Tantillo, *Am. Sci.* **2019**, *107*, 22–26.
[13] a) P. M. Hoffman, *Life's Ratchet. How Molecular Machines Extract Order from Chaos*, Basic Books, New York **2012**; b) M. N. Chatterjee, E. R. Kay, D. A. Leigh, *J. Am. Chem. Soc.* **2006**, *128*, 4058–4073.
[14] a) R. D. Astumian, *Science* **1997**, *276*, 917–922; b) R. D. Astumian, *Phys. Chem. Chem. Phys.* **2007**, *9*, 5067–5083.
[15] a) L. Onsager, *Phys. Rev.* **1931**, *37*, 405–426; b) D. G. Blackmond, *Angew. Chem., Int. Ed.* **2009**, *48*, 2648–2654; c) R. D. Astumian, *Nature Nanotech.* **2012**, *7*, 684–688.
[16] R. D. Astumian, M. Bier, *Biophys. J.* **1996**, *70*, 637–653.
[17] R. D. Astumian, *Faraday Discuss.* **2016**, *195*, 583–597.
[18] T. Sangchai, S. Al Shehimy, E. Penocchio, G. Ragazzon, *Angew. Chem., Int. Ed.* **2023**, *62*, e202309501.
[19] V. Balzani, N. Armaroli, *Energy for a Sustainable World: From the Oil Age to a Sun-Powered Future*, Wiley, Weinheim **2011**.
[20] a) S. Corra, M. Curcio, M. Baroncini, S. Silvi, A. Credi, *Adv. Mater.* **2020**, *32*, 1906064; b) M. Baroncini, J. Groppi, S. Corra, S. Silvi, A. Credi, *Adv. Optical Mater.* **2019**, *7*, 1900392; c) S. Corra, M. Curcio, A. Credi, *JACS Au* **2023**, *3*, 1301–1313.
[21] V. Balzani, M. Clemente-León, A. Credi, B. Ferrer, M. Venturi, A. H. Flood, J. F. Stoddart, *Proc. Natl. Acad. Sci. USA* **2006**, *103*, 1178–1183.
[22] a) S. S. Correa, J. Schultz, K. J. Lauersen, A. S. Rosado, *J. Adv. Res.* **2023**, *47*, 75–92; b) K. P. Hofmann, T. D. Lamb, *Prog. Retinal Eye Res.* **2023**, *93*, 101116.
[23] E. J. Bowen, *The Chemical Aspects of Light*, Clarendon Press, **1946**.
[24] E. Penocchio, R. Rao, M. Esposito, *J. Chem. Phys.* **2021**, *155*, 114101.
[25] a) R. T. Ross, *J. Chem. Phys.* **1966**, *45*, 1–7; b) G. Porter, *J. Chem. Soc., Faraday Trans. 2* **1983**, *79*, 473–482.
[26] A. Einstein, *Dtsch. Phys. Ges.* **1916**, *18*, 318–323.
[27] N. Koumura, R. W. J. Zijlstra, R. A. van Delden, N. Harada, B. L. Feringa, *Nature* **1999**, *401*, 152–155.
[28] R. S. H. Liu, *Acc. Chem. Res.* **2001**, *34*, 555–562.
[29] A. Gerwien, M. Schildhauer, S. Thumser, P. Mayer, H. Dube, *Nat. Commun.* **2018**, *9*, 2510.
[30] a) J.-M. Lehn, *Chem. Eur. J.* **2006**, *12*, 5910–5915; b) L. Greb, J.-M. Lehn, *J. Am. Chem. Soc.* **2014**, *136*, 13114–13117; c) L. Greb, A. Eichhofer, J.-M. Lehn, *Angew. Chem., Int. Ed.* **2015**, *54*, 14345–14348.
[31] M. Filatov(Gulak), M. Paolino, R. Pierron, A. Cappelli, G. Giorgi, J. Léonard, M. Huix-Rotllant, N. Ferré, X. Yang, D. Kaliakin, A. Blanco-González, M. Olivucci, *Nat. Commun.* **2022**, *13*, 6433.
[32] a) M. Guentner, M. Schildhauer, S. Thumser, P. Mayer, D. Stephenson, P. J. Mayer, H. Dube, *Nat. Commun.* **2015**, *6*, 8406; b) A. Gerwien, P. Mayer, H. Dube, *J. Am. Chem. Soc.* **2018**, *140*, 16442–16445; c) A. Gerwien, P. Mayer, H. Dube, *Nat. Commun.* **2019**, *10*, 4449; d) A. Gerwien, F. Gnannt, P. Mayer, H. Dube, *Nat. Chem.* **2022**, *14*, 670–676.
[33] a) For the rate laws used to define the rate terms ("ri") in eq. 1 we refer the reader to the following references: M. Montalti, A. Credi, L. Prodi, M. T. Gandolfi, *Handbook of Photochemistry*, CRC Press, Boca Raton, Florida, **2006**; b) P. Klán, J. Wirz, *Photochemistry of Organic Compounds: From Concepts to Practice*, Wiley, Hoboken, New Jersey, **2009**; c) M. Feinberg, *Foundations of Chemical Reaction Network Theory*, Springer, New York City, New York, **2019**.
[34] Equation 2 could be rearranged taking into account the Einstein relations for absorption and emission of light. While this is outside of the scope of the current review, we refer the reader to ref. [17] or [24].
[35] W. Hwang, M. Karplus, *Proc. Natl. Acad. Sci. USA* **2019**, *116*, 19777–19785.
[36] a) D. R. S. Pooler, A. S. Lubbe, S. Crespi, B. L. Feringa, *Chem. Sci.* **2021**, *12*, 14964–14986; b) D. Rokea, S. J. Wezenberg, B. L. Feringa, *Proc. Natl. Acad. Sci. USA* **2018**, *115*, 9423–9431.
[37] G. S. Kottas, L. I. Clarke, D. Horinek, J. Michl, *Chem. Rev.* **2005**, *105*, 1281–1376.
[38] S. Corra, M. Tranfić-Bakić, J. Groppi, M. Baroncini, S. Silvi, E. Penocchio, M. Esposito, A. Credi, *Nat. Nanotechnol.* **2022**, *17*, 746–751.
[39] The term "rotor" has been often used as a synonym for "rotator". This, however, may give rise to ambiguity since "rotor" can also be referred to the entire molecule. Within this review we have consistently adopted the term "rotator" according to Michl's definition (ref. [37]).
[40] a) C. R. Hall, J. Conyard, I. A. Heisler, G. Jones, J. Frost, W. R. Browne, B. L. Feringa, S. R. Meech, *J. Am. Chem. Soc.* **2017**, *139*, 7408–7414; b) C. R. Hall, W. R. Browne, B. L. Feringa, S. R. Meech, *Angew. Chem., Int. Ed.* **2018**, *57*, 6203–6207.
[41] J. Conyard, K. Addison, I. A. Heisler, A. Cnossen, W. R. Browne, B. L. Feringa, S. R. Meech *Nature Chem.* **2012**, *4*, 547–551.
[42] a) J. Sheng, W. Danowski, A. S. Sardjan, J. Hou, S. Crespi, A. Ryabchun, M. P. Domínguez, W. J. Buma, W. R. Browne, B. L. Feringa, *Nat. Chem.* **2024**, *16*, 1330–1338; b) J. Shen, C. L. F. van Beek, C. N. Stindt, W. Danowski, J. Jankowska, S. Crespi, D. R. S. Pooler, M. F. Hilbers, W. Jan Buma, B. L. Feringa, *Sci. Adv.* **2025**, *11*, eadr9326.
[43] a) C. Gao, A. V. Jentzsch, E. Moulin, N. Giuseppone, *J. Am. Chem. Soc.* **2022**, *144*, 9845–9852; b) M. Kathan, S. Crespi, N. O. Thiel, D. L. Stares, D. Morsa, J. de Boer, G. Pacella, T. van den Enk, P. Kobauri, G. Portale, C. A. Schalley, B. L. Feringa, *Nat. Nanotechnol.* **2022**, *17*, 159–165.
[44] a) Q. Li, G. Fuks, E. Moulin, M. Maaloum, M. Rawiso, I. Kulic, T. J. Foy, N. Giuseppone, *Nat. Nanotechnol.* **2015**, *10*, 161–165; b) J. T. Foy, Q. Li, A. Goujon, J.-R. Colard-Itté, G. Fuks, E. Moulin, O. Schiffmann, D. Dattler, D. P. Funeriu, N. Giuseppone, *Nat. Nanotechnol.* **2017**, *12*, 540–545; c) A. Perrot, W. Wang, E. Buhler, E. Moulin, N. Giuseppone, *Angew. Chem., Int. Ed.* **2023**, *62*, e202300263.
[45] S. Chen, L. Yang, F. K.-C. Leung, T. Kajitani, M. C. A. Stuart, T. Fukushima, P. van Rijn, B. L. Feringa, *J. Am. Chem. Soc.* **2022**, *144*, 3543–3553.
[46] a) W.-Z. Wang, L.-B. Huang, S.-P. Zheng, E. Moulin, O. Gavat, M. Barboiu, N. Giuseppone, *J. Am. Chem. Soc.* **2021**, *143*, 15653–15660; b) H. Yang, J. Yi, S. Pang, K. Ye, Z. Ye, Q. Duan, Z. Yan, C. Lian, Y. Yang, L. Zhu, D.-H. Qu, C. Bao, *Angew. Chem., Int. Ed.* **2022**, *61*, e202204605.
[47] V. García-López, F. Chen, L. G. Nilewski, G. Duret, A. Aliyan, A. B. Kolomeisky, J. T. Robinson, G. Wang, R. Pal, J. Tour, *Nature* **2017**, *548*, 567–572.
[48] a) T. S. C. MacDonald, W. S. Price, R. D. Astumian, J. E. Beves, *Angew. Chem., Int. Ed.* **2019**, *58*, 18864–18867; b) A. M. Firsov, J. Pfeffermann, A. S. Benditkis, T. I. Rokitskaya, A. S. Kozlov, E. A. Kotova, A. A. Krasnovsky, P. Pohl, Y. N. J. Antonenko, *Photochem. Photobiol. B* **2023**, *239*, 112633; c) J. L. Beckham, T. S. Bradford, C. Ayala-Orozco, A. L. Santos, D. Arnold, A. R. van Venrooy, V. García-López, R. Pal, J. M. Tour, *Adv. Mater.* **2024**, *36*, 2306669.
[49] P. Štacko, J. C. M. Kistemaker, T. van Leeuwen, M.-C. Chang, E. Otten, B. L. Feringa, *Science* **2017**, *356*, 964–968.
[50] Y. Gisbert, M. Ovalle, C. N. Stindt, R. Costil, B. L. Feringa, *Angew. Chem., Int. Ed.* **2025**, *64*, e202416097.

[51] M. Guentner, M. Schildhauer, S. Thumser, P. Mayer, D. Stephenson, P. J. Mayer, H. Dube, *Nat. Commun.* **2015**, *6*, 8406.
[52] F. Gnannt, A. Gerwien, S. Waldmannstetter, S. Gracheva, H. Dube, *Angew. Chem., Int. Ed.* **2024**, *136*, e202405299.
[53] a) A. Blokhuis, R. Pollice, *Eur. J. Org. Chem.* **2025**, *28*, e202400949; b) R. Deka, J. D. Steen, M. F. Hilbers, W. G. Roeterdink, A. Iagatti, R. Xiong, W. J. Buma, M. Di Donato, A. Orthaber, S. Crespi, *Angew. Chem., Int. Ed.* **2025**, *64*, e202419943.
[54] B. L. Regen-Pregizer, A. Ozcelik, P. Mayer, F. Hampel, H. Dube, *Nat. Commun.* **2023**, *14*, 4595.
[55] L. Reißenweber, E. Uhl, F. Hampel, P. Mayer, H. Dube, *J. Am. Chem. Soc.* **2024**, *146*, 23387–23397.
[56] B. L. Regen-Pregizer, H. Dube, *J. Am. Chem. Soc.* **2023**, *145*, 13081–13088.
[57] D. Roke, M. Sen, W. Danowski, S. J. Wezenberg, B. L. Feringa, *J. Am. Chem. Soc.* **2019**, *141*, 7622–7627.
[58] D. R. S. Pooler, R. Pierron, S. Crespi, R. Costil, L. Pfeifer, J. Léonard, M. Olivucci, B. L. Feringa, *Chem. Sci.* **2021**, *12*, 7486–7497.
[59] D. R. S. Pooler, D. Doellerer, S. Crespi, B. L. Feringa, *Org. Chem. Front.* **2022**, *9*, 2084–2092.
[60] A. Guinart, D. Doellerer, D. R. S. Pooler, J. Y. de Boer, S. Doria, L. Bussotti, M. Di Donato, B. L. Feringa, *J. Photochem. Photobiol. A* **2024**, *453*, 115649.
[61] L. Liu, W.-H. Fang, T. J. Martinez, *J. Am. Chem. Soc.* **2023**, *145*, 6888–6898.
[62] K. Kuntze, D. R. S. Pooler, M. Di Donato, M. F. Hilbers, P. van der Meulen, J. B. Wybren, A. Priimagi, B. L. Feringa, S. Crespi, *Chem. Sci.* **2023**, *14*, 8458–8465.
[63] F. Nicoli, C. Taticchi, E. Lorini, S. Borghi, F. Aleotti, S. Silvi, A. Credi, M. Garavelli, L. Muccioli, M. Baroncini, M. Curcio, *ChemRxiv preprint* **2024**, https://doi.org/10.26434/chemrxiv-2024-03sk0.
[64] V. Serreli, C.-F. Lee, E. R. Kay, D. A. Leigh, *Nature* **2007**, *445*, 523–527.
[65] H. Li, C. Cheng, P. R. McGonigal, A. C. Fahrenbach, M. Frasconi, W.-G. Liu, Z. Zhu, Y. Zhao, C. Ke, J. Lei, R. M. Young, S. M. Dyar, D. T. Co, Y.-W. Yang, Y. Y. Botros, W. A. Goddard III, M. R. Wasielewski, R. D. Astumian, J. F. Stoddart, *J. Am. Chem. Soc.* **2013**, *135*, 18609–18620.
[66] G. Ragazzon, M. Baroncini, S. Silvi, M. Venturi, A. Credi, *Nat. Nanotechnol.* **2015**, *10*, 70–75.
[67] a) L. Casimiro, J. Groppi, M. Baroncini, M. La Rosa, A. Credi, S. Silvi, *Photochem. Photobiol. Sci.* **2018**, *17*, 734–740; b) J. Groppi, L. Casimiro, M. Canton, S. Corra, M. Jafari-Nasab, G. Tabacchi, L. Cavallo, M. Baroncini, S. Silvi, E. Fois, A. Credi, *Angew. Chem., Int. Ed.* **2020**, *59*, 14825–14834; c) S. Corra, L. Casimiro, M. Baroncini, J. Groppi, M. La Rosa, M. Tranfić Bakić, S. Silvi, A. Credi, *Chem. Eur. J.* **2021**, *27*, 11076–11083; d) M. Canton, J. Groppi, L. Casimiro, S. Corra, M. Baroncini, S. Silvi, A. Credi, *J. Am. Chem. Soc.* **2021**, *143*, 10890–10894.
[68] A. Sabatino, E. Penocchio, G. Ragazzon, A. Credi, D. Frezzato, *Angew. Chem., Int. Ed.* **2019**, *58*, 14341–14348.
[69] F. Nicoli, M. Curcio, M. Tranfic Bakic, E. Paltrinieri, S. Silvi, M. Baroncini, A. Credi, *J. Am. Chem. Soc.* **2022**, *144*, 10180–10185.
[70] a) G. Ragazzon, L. J. Prins, *Nature Nanotech.* **2018**, *13*, 882–889; b) S. Amano, S. Borsley, D. A. Leigh, Z. Sun, *Nat. Nanotechnol.* **2021**, *16*, 1057–1067.
[71] S. Borsley, D. A. Leigh, B. M. W. Roberts, *Angew. Chem., Int. Ed.* **2024**, *63*, e202400495.
[72] S. Amano, M. Esposito, E. Kreidt, D. A. Leigh, E. Penocchio, B. M. W. Roberts, *J. Am. Chem. Soc.* **2022** *144*, 20153–20164.
[73] A. I. Brown, D. A. Sivak, *Chem. Rev.* **2020**, *120*, 434–459.
[74] R. D. Astumian, *Nat. Commun.* **2019**, *10*, 3837.
[75] E. Penocchio, G. Gu, A. Albaugh, T. R. Gingrich, *J. Am. Chem. Soc.* **2024**, *147*, 1063–1073.
[76] L. Binks, S. Borsley, T. R. Gingrich, D. A. Leigh, E. Penocchio, B. M. W. Roberts, *Chem* **2023**, *9*, 2902–2917.
[77] S. Borsley, D. A. Leigh, B. M. W. Roberts, *Nat. Chem.* **2022**, *14*, 728–738.
[78] K. Kazuhiko, Y. Ryohei, N. Hiroyuki, A. Kengo, *Phil. Trans. R. Soc. Lond. B* **2000**, *355*, 473–489.
[79] T. Marchetti, B. M. W. Roberts, D. Frezzato, L. J. Prins, *Angew. Chem., Int. Ed.* **2024**, *63*, e202402965.
[80] S. A. P. van Rossum, M. Tena-Solsona, J. H. van Esch, R. Eelkema, J. Boekhoven, *Chem. Soc. Rev.* **2017**, *46*, 5519–5535.
[81] a) T. R. Kelly, I. Tellitu, J. P. Sestelo, *Angew. Chem. Int. Ed. Engl.* **1997**, *36*, 1866–1868; b) T. R. Kelly, H. De Silva, R. A. Silva, *Nature* **1999**, *401* 150–152; c) T. R. Kelly, X. Cai, F. Damkaci, S. B. Panicker, B. Tu, S. M. Bushell, I. Cornella, M. J. Piggott, R. Salives, M. Cavero, Y. Zhao, S. Jasmin, *J. Am. Chem. Soc.* **2007**, *129*, 376–386.
[82] M. R. Wilson, J. Solà, A. Carlone, S. M. Goldup, N. Lebrasseur, D. A. Leigh, *Nature* **2016**, *534*, 235–240.
[83] A. Albaugh, T. R. Gingrich, *Nat. Commun.* **2022**, *13*, 2204.
[84] S. Amano, M. Esposito, E. Kreidt, D. A. Leigh, E. Penocchio, B. M. W. Roberts, *Nat. Chem.* **2022**, *14*, 530–537.
[85] S. Borsley, D. A. Leigh, B. M. W. Roberts, *J. Am. Chem. Soc.* **2021**, *143*, 4414–4420.
[86] S. Borsley, E. Kreidt, D. A. Leigh, B. M. W. Roberts, *Nature* **2022**, *604*, 80–85.
[87] P.-L. Wang, S. Borsley, M. J. Power, A. Cavasso, N. Giuseppone, D. A. Leigh, *Nature* **2025**, *637*, 594–600.
[88] S. Borsley, D. A. Leigh, B. M. W. Roberts, I. J. Vitorica-Yrezabal, *J. Am. Chem. Soc.* **2022**, *144*, 17241–17248.
[89] J. M. Gallagher, B. M. W. Roberts, S. Borsley, D. A. Leigh, *Chem* **2024**, *10*, 855–866.
[90] S. Amano, S. D. P. Fielden, D. A. Leigh, *Nature* **2021**, *594*, 529–534.
[91] S. D. P. Fielden, *ChemSystemsChem* **2024**, *6*, e202300048.
[92] L. Binks, C. Tian, S. D. P. Fielden, I. J. Vitorica-Yrezabal, D. A. Leigh, *J. Am. Chem. Soc.* **2022**, *144*, 15838–15844.
[93] a) G. Steinberg-Yfrach, P. Liddell, S. C. Hung, A. L. Moore, D. Gust, T. A. Moore, *Nature* **1997**, *385*, 239–241; b) G. Steinberg-Yfrach, J.-L. Rigaud, E. N. Durantini, A. L. Moore, D. Gust, T. A. Moore, *Nature* **1998**, *392*, 479–482; c) I. M. Bennett, H. M. Vanegas Farfano, F. Bogani, A. Primak, P. A. Liddell, L. Otero, L. Sereno, J. J. Silber, A. L. Moore, T. A. Moore, D. Gust, *Nature* **2002**, *420*, 398–401; d) E. N. W. Howe, P. A. Gale, *J. Am. Chem. Soc.* **2019**, *141*, 10654–10660.
[94] a) X. Xie, G. A. Crespo, G. Mistlberger, E. Bakker, *Nature Chem.* **2014**, *6*, 202–207; b) J. Pruchyathamkorn, B.-N. T. Nguyen, A. B. Grommet, M. Novoveska, T. K. Ronson, J. D. Thoburn, J. R. Nitschke, *Nature Chem.* **2024**, *16*, 1558–1564; c) B. Shao, H. Fu, I. Aprahamian, *Science* **2024**, *385*, 544–549.
[95] A.-K. Pumm, W. Engelen, E. Kopperger, J. Isensee, M. Vogt, V. Kozina, M. Kube, M. N. Honemann, E. Bertosin, M. Langecker, R. Golestanian, F. C. Simmel, H. Dietz, *Nature* **2022**, *607*, 492–498.

Manuscript received: December 23, 2024
Revised manuscript received: March 28, 2025
Version of record online: April 28, 2025